

# A new species of *Largocephalosaurus* (Diapsida: Saurosphargidae), with implications for the morphological diversity and phylogeny of the group

CHUN LI\*†, DA-YONG JIANG‡, LONG CHENG§, XIAO-CHUN WU†¶  
& OLIVIER RIEPPEL||

\*Laboratory of Evolutionary Systematics of Vertebrates, Institute of Vertebrate Paleontology and Paleoanthropology, Chinese Academy of Sciences, PO Box 643, Beijing 100044, China

‡Department of Geology and Geological Museum, Peking University, Beijing 100871, PR China

§Wuhan Institute of Geology and Mineral Resources, Wuhan, 430223, PR China

¶Canadian Museum of Nature, PO Box 3443, STN 'D', Ottawa, ON K1P 6P4, Canada

||Department of Geology, The Field Museum, 1400 S. Lake Shore Drive, Chicago, IL 60605-2496, USA

(Received 31 July 2012; accepted 25 February 2013)

**Abstract** – *Largocephalosaurus polycarpon* Cheng *et al.* 2012a was erected after the study of the skull and some parts of a skeleton and considered to be an eosauropterygian. Here we describe a new species of the genus, *Largocephalosaurus qianensis*, based on three specimens. The new species provides many anatomical details which were described only briefly or not at all in the type species, and clearly indicates that *Largocephalosaurus* is a saurosphargid. It differs from the type species mainly in having three premaxillary teeth, a very short retroarticular process, a large pineal foramen, two sacral vertebrae, and elongated small granular osteoderms mixed with some large ones along the lateral most side of the body. With additional information from the new species, we revise the diagnosis and the phylogenetic relationships of *Largocephalosaurus* and clarify a set of diagnostic features for the Saurosphargidae Li *et al.* 2011. *Largocephalosaurus* is characterized primarily by an oval supratemporal fenestra, an elongate dorsal 'rib-basket', a narrow and elongate transverse process of the dorsal vertebrae, and the lack of a complete dorsal carapace of osteoderms. The Saurosphargidae is distinct mainly in having a retracted external naris, a jugal–squamosal contact, a large supratemporal extensively contacting the quadrate shaft, a leaf-like tooth crown with convex labial surface and concave lingual surface, a closed dorsal 'rib-basket', many dorsal osteoderms, a large boomerang-like or atypical T-shaped interclavicle. Current evidence suggests that the Saurosphargidae is the sister-group of the Sauropterygia and that *Largocephalosaurus* is the sister-group of the *Saurosphargis*–*Sinosaurosphargis* clade within the family.

Keywords: marine reptile, morphology, phylogeny, Triassic, China.

## 1. Introduction

The marine vertebrate fauna of the Triassic Guanling Formation has become well known recently, occurring mainly in boundary area between Yunnan and Guizhou provinces in southwestern China (Jiang *et al.* 2006; 2008, 2009; Motani *et al.* 2008; Wang *et al.* 2009; Wu *et al.* 2011; Liu *et al.* 2011; Shang, Wu & Li, 2011). Conodonts dated the fossil yielding strata (Upper Member) of the Guanling Formation to the Pelsonian substage of the Anisian, Middle Triassic (Sun *et al.* 2006; Zhang *et al.* 2009). This fauna has been recently enriched by the discovery of a new member, *Sinosaurosphargis yunguiensis* Li *et al.* 2011, of the Saurosphargidae Li *et al.* 2011 from Luoping County, Yunnan. Early in 2012, a new marine reptile, *Largocephalosaurus polycarpon* Cheng *et al.* 2012a was briefly described and attributed to the Eosauropterygia. Our further examination of the specimen suggests that this reptile is most probably referable to

the Saurosphargidae and represents a new morphotype of the family. This is supported by the discovery of a new species *Largocephalosaurus qianensis* (see Section 3) from the same horizon of southwestern Guizhou, about 100 km northeast of the type locality of *L. polycarpon* in Luoping County, Yunnan.

*L. polycarpon* was originally established primarily based on an incomplete skull because the preparation of the postcranial skeleton of the specimen, WIGM (Wuhan Institute of Geology and Mineral Resources) SPC V 1009, was then incomplete. It was considered to be an eosauropterygian and closely related to the Nothosauroidae–Pachypleurosauria clade within the Sauropterygia (Cheng *et al.* 2012a). Whilst this specimen was being studied, research groups at GMPKU (Geological Museum of Peking University) and IVPP (Institute of Vertebrate Paleontology and Paleoanthropology, Chinese Academy of Sciences) were working on three similar specimens collected from the Upper Member of the Guanling Formation in Panxian, Guizhou Province in 2008. The GMPKU specimen was briefly reported as *Saurosphargis* cf.

†Authors for correspondence: lichun@ivpp.ac.cn; xwu@mus-nature.ca

*S. volzi* (Jiang *et al.* 2011). These new specimens are better preserved than that of the type species, and clearly show the presence of dorsal osteoderms and a closed dorsal 'rib-basket' formed by the underlying ribs. Our further examination demonstrates that those features are also present in *L. polycarpon* as shown by the partly prepared postcranial skeleton. Therefore, it is evident that *Largocephalosaurus* is clearly not an eosauroptrygian but instead may be closely related to the Saurosphargidae. In morphology, the three new specimens are different enough from *L. polycarpon* and represent a new species; the most striking of those differences are: the presence of three premaxillary teeth, an oval orbit, a large parietal foramen, two (rather than three) sacral vertebrae, a unique pattern of osteoderms, and a short retroarticular process. Here, we describe the osteological anatomy of the new species, revise the systematics of *Largocephalosaurus*, and further test the phylogenetic relationships of the Saurosphargidae with other marine reptilian groups.

## 2. Material and methods

All three specimens were preserved in blocks of limestone or muddy limestone. One is a nearly complete skeleton, housed at the IVPP. As for the other two specimens housed at the GMPKU, one is represented by a skull and a cervical vertebra and the other is an incomplete skeleton with the skull and most of the tail missing. All specimens were mechanically prepared using aircsribes with tips of various sizes. The IVPP specimen was exposed in ventral view but its skull was prepared on both dorsal and ventral sides. The two GMPKU specimens were exposed only in dorsal view.

## 3. Systematic palaeontology

Order DIAPSIDA Osborn, 1903  
Family SAUROSPHARGIDAE Li *et al.* 2011

*Type genus.* *Saurosphargis* Huene, 1936.

*Referred genera.* *Sinosaurosphargis* Li *et al.* 2011; *Largocephalosaurus* Cheng *et al.* 2012a (originally described as an eosauroptrygian).

*Diagnosis.* Aquatic diapsids characterized by the following combination of apomorphies: (1) dorsal ribs forming a closed basket; (2) presence of dorsal osteoderms; (3) external naris retracted, much closer to orbit than rostral tip; (4) median elements of gastral ribs often with a two-pronged lateral process on one side; (5) lateral most elements of gastral ribs broadened and contacting each other; (6) supratemporal extensively contacting quadrate shaft; (7) posterior margin of skull roof deeply emarginated; (8) jugal-squamosal contact; (9) presence of ectopterygoid; (10) presence of interpterygoid vacuity and open braincase-palatal articulation; (11) leaf-shaped tooth crown with convex labial surface and concave lingual surface; (12) dorsal vertebrae with elongate transverse process and a very low neural spine; (13) tip of neural spines table-like, covered by osteoderm(s); (14) large interclavicle boomerang-like or atypical T-shaped, with a small and sharp posterior process;

(15) humerus not expanded at both ends; (16) nine carpals; and (17) four tarsals.

*Remarks.* *Saurosphargis*, the type genus of the Saurosphargidae, from the Middle Triassic of Europe, is a poorly known taxon; it is only represented by a section of 12 incomplete dorsal vertebrae with ribs (see Nosotti & Rieppel, 2003, fig. 11). The diagnosis of the family was not defined when the family was established and is here largely based on two Chinese genera: *Sinosaurosphargis* and *Largocephalosaurus*.

*Largocephalosaurus* Cheng *et al.* 2012a

*Type species.* *Largocephalosaurus polycarpon* Cheng *et al.* 2012a.

*Revised diagnosis.* A saurosphargid genus differing from the others of the family in the following combination of apomorphies: (1) closed dorsal 'rib-basket' elongate oval; (2) oval supratemporal fenestra present, much smaller than orbit; (3) premaxilla excluded from external naris; (4) three or four premaxillary teeth; (5) posterolateral process of frontal elongate; (6) transverse process of dorsal vertebrae and proximal portion of the dorsal ribs slender, not much wider than inter-process or inter-rib spaces, respectively; (7) presence of a median row of large osteoderms on the top of neural spines; (8) coracoid and pubis similarly round in outline, separately with an open coracoid foramen and an open obturator fenestra; and (9) dorsal osteoderms not forming a complete carapace.

*Remarks.* Most of the diagnostic characters for *Largocephalosaurus* are unknown in *Saurosphargis* owing to the fragmentary nature of the latter. However, characters (1) and (6) distinguish the two genera. In *Saurosphargis* the body should have been broader than in *Largocephalosaurus* in terms of a large turning angle at the shoulder region of the dorsal ribs; this condition is comparable to that of *Sinosaurosphargis*. Similarly, the transverse process of the dorsal vertebrae and the proximal (dorsal) portion of the dorsal ribs are very similar between *Saurosphargis* and *Sinosaurosphargis* in morphology; they are much broader than the inter-process or inter-rib spaces.

*Largocephalosaurus qianensis* sp. nov.  
Figures 1, 2, 3, 4a–g, 5a–d, 6

*Etymology.* Specific name refers to the simplified name 'Qian' for Guizhou Province where the specimens were collected.

*Holotype.* IVPP V 15638, a nearly complete skeleton in ventral view, with posterior-most section of the tail missing.

*Referred specimens.* GMPKU-P-1532-A, a skull with a cervical vertebra in dorsal view. GMPKU-P-1532-B, an incomplete postcranial skeleton in dorsal view, with the posterior portion of the mandible but missing most of the tail.

*Type locality and horizon.* Xinmin District, Panxian County, southwest-most Guizhou Province, P. R. China; Member II of the Guanling Formation, Anisian, Middle Triassic.

*Referred locality and horizon.* As for the type.

*Diagnosis.* Differing from the type species in the following characters: (1) parietal paired; (2) pineal foramen large;

(3) orbit oval in outline; (4) a distinct palatal fossa on the dorsal surface of palatine; (5) dorsal osteoderms elongated granular in outline and covering the lateral side of body, mixed with large and nearly round ones; (6) retroarticular process very short; (7) shoulder portion of dorsal ribs with no crest on dorsal surface but broadening as an uncinat-like process; (8) 33 presacral vertebrae (including 24 dorsals); and (9) two sacral vertebrae.

**Remarks.** The genotype species, *L. polycarpon*, has not been fully described because the preparation of the postcranial skeleton was not completed when it was erected. A number of characters listed in the diagnosis of the new species were recognized on the basis of the comparison with the partly prepared skeleton of the type species. A full description of *L. polycarpon* is in preparation.

#### 4. Morphological description

The following description is based on IVPP V 15638 (the type specimen) unless the referred specimens (GMPKU-P-1532-A and GMPKU-P-1532-B) are identified.

##### 4.a. Skull and mandible

The skull is dorsoventrally compressed. The fronto-parietal skull table is well preserved in both IVPP V 15638 and GMPKU-P-1532-A. The region around the external nares is badly crushed in the former (Fig. 1c, d), but it is relatively better preserved in the latter (Fig. 2a, b). The rostrum, mainly formed by the premaxillae, is distinct and anteriorly rounded with parallel lateral margins as in *Sinosauropsphargis*. Posterior to the premaxilla–maxillary suture, the skull gradually widens, reaching its maximum width at the point between the posterior third of the orbits; the latter are of oval contour in lateral view, differing from the round outline in the type species (Cheng *et al.* 2012a, fig. 2). The orbital margins form a thickened, granulated rim as in *Sinosauropsphargis* (Li *et al.* 2011, fig. 2A). Our observations suggest that the smooth orbital margins of the type species are not original but a result of surficial erosion. The supratemporal fenestra remains open but is small, reaching a size of less than half that of the orbits, as in the type species. The pineal foramen is located anteriorly on the parietal skull table as in *Sinosauropsphargis* but much larger than in the latter, and even larger than that of the type species. The ventral cheek region may have been deeply embayed in life, suggesting a large infratemporal fenestra as in *Sinosauropsphargis* and *Hanosaurus* (Rieppel, 1998a, fig. 2) although it is obscured by the dorsoventral compression of the skull. The posterior margin of the skull roof is strongly emarginated, showing a deep V-shaped outline. The braincase is obscured by the extensive overlap of the skull roof bones, which has been further exaggerated by the displacement of the relevant elements owing to the dorsoventral compression (for skull measurements see Table 1).

The paired premaxillae are relatively large as in many of the other aquatic sauropterygians (Rieppel, 2000a). Their dorsal surface around the rostral end is distinctly granulated, but pitted and grooved in other areas. The palatal surface of the rostrum is not exposed. The premaxilla, as shown in GMPKU-P-1532-A, is excluded by the anterior maxilla–nasal contact from the margin of the external naris (Fig. 2a, b), as in the type species; in contrast, no such a maxilla–nasal contact separates the bone from the naris in *Sinosauropsphargis*. The premaxilla meets the maxilla in the ventral margin of the upper jaw far posterior to the anterior end of the rostrum as in the latter, but the suture of the

two bones is gently curved, extending posterodorsally as in the type species. The premaxilla bears only three teeth, unlike four teeth reported for the type species, five or six in *Sinosauropsphargis*, or five preserved in *Eusauropsphargis*, a similar aquatic reptile (Nosotti & Rieppel, 2003); all three teeth are *in situ* on the left side but there are two plus an alveolus on the right side (Fig. 3a, b). The teeth are implanted in shallow sockets, in a sub-thecodont pattern. The tooth morphology is similar to that of *Sinosauropsphargis* (Li *et al.* 2011, fig. 2E) and *Eusauropsphargis* (Nosotti & Rieppel, 2003, fig. 3), with a basally expanded crown that is set off from a distinctly waisted peduncle and striations on the labial surface of the crown. The monocuspid tooth crown has a convex labial and a strongly concave lingual surface covered by striated enamel. In GMPKU-P-1532-A, the anterior-most tooth of the left premaxilla is exposed and the three teeth of the right premaxillary are also visible in dorsal view although none of them is complete (Fig. 2a, b). Our examination indicates that none of the preserved teeth is complete in the type species and the description of the tooth morphology for the species was not accurate. Striations and a waisted peduncle traceable in some teeth suggest that the type species most probably had similar tooth morphology.

The nasals of GMPKU-P-1532-A are complete and similar to those of the type species. They form a pair of rather large, plate-like elements that are slightly shorter but broader in the mid portion than the frontals (Fig. 2a, b). The nasal becomes narrower at both anterior and posterior ends. It forms the posterior and much of the dorsal margins of the external naris. Laterally, the strongly expanded mid-part meets the ascending (facial) process of the maxilla. Posterolaterally, the nasal-prefrontal suture is simple, convex towards the nasal. Posteriorly, the nasal–frontal suture is interdigitating. The dorsal surface of the nasals is distinctly grooved and ridged; the grooves and ridges are arranged in longitudinal rows on the posterior part of the bone.

The paired frontals contribute, compared with those of *Sinosauropsphargis*, a smaller part to the dorsal margin of the orbit. The broader contribution of the bone to the orbit in the type species may be not true because surface erosion has obscured the sutural patterns of the frontal with the neighbouring elements. Laterally, the frontal contacts the prefrontal anteriorly and the postfrontal posteriorly. Posteriorly, the frontal forms an elongate process that extends posteriorly and slightly laterally beyond the pineal foramen and approaches the supratemporal fenestra, as in the type species. This results in strongly concave posterior margins of the frontals and deeply interdigitating fronto-parietal sutures. Such a process is commonly present in European pachypleurosaurs such as *Neusticosaurus* and *Serpianosaurus* (Carroll & Gaskill, 1985; Sander, 1989; Rieppel, 1989) or the pachypleurosaurs-like Chinese forms such as *Wumengosaurus* (Wu *et al.* 2011) and *Diandongosaurus* (Shang, Wu & Li, 2011) but not in *Sinosauropsphargis*. The dorsal surface of the frontals shows grooves and ridges arranged in a similar pattern to that seen in the nasals.

The parietals are paired (Figs 1b, c; 2a, b); unlike the type species in which they are fused posterior to the pineal foramen, or *Sinosauropsphargis* where they are entirely fused. The parietals form narrow anterior processes inserting into the frontals; each has a small anterolateral process to meet the postfrontal along the anteromedial margin of the supratemporal fenestra. The parietal broadens between the supratemporal fenestrae. Posterior to the end of the dorsal midline, the parietal forms a short posterolateral process along the deeply excavated occipital edge as in the type species which is different from the condition seen in

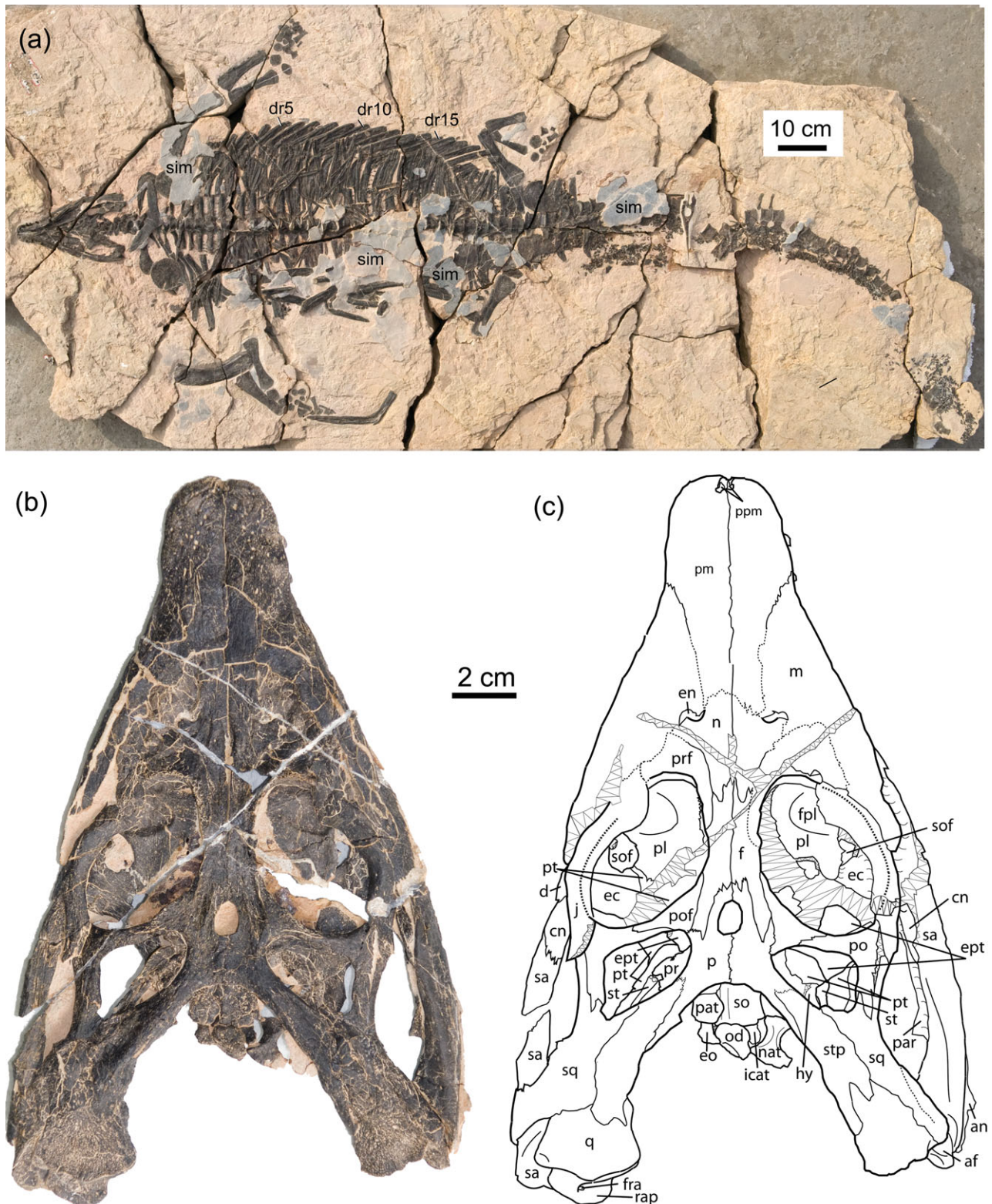


Figure 1. (Colour online) Type specimen of *Largocephalosaurus qianensis* sp. nov. (IVPP V 15638). (a) Skeleton in ventral view; (b) skull and mandible in dorsal view; (c) line drawing of (b). Abbreviations: af – articular fossa; an – angular; cn – coronoid; d – dentary; dr – dorsal rib; ec – ectopterygoid; en – external naris; eo – exoccipital; ept – epipterygoid; f – frontal; fpl – fossa on palatine; fra – foramen on retroarticular process; hy – hyoid; icat – atlantal intercentrum; j – jugal; m – maxilla; n – nasal; nat – neural arch of atlas; od – odontoid process; p – parietal; par – prearticular; pat – proatlas; pl – palatine; pm – premaxilla; po – postorbital; pof – postfrontal; ppm – palatal portion of premaxilla; pr – prootic; prf – prefrontal; pt – pterygoid; q – quadrate; rap – retroarticular process; sa – surangular; sim – possible skin impression; so, supraoccipital; sof – suborbital fenestra; sq – squamosal; st – stapes; stp – supratemporal.

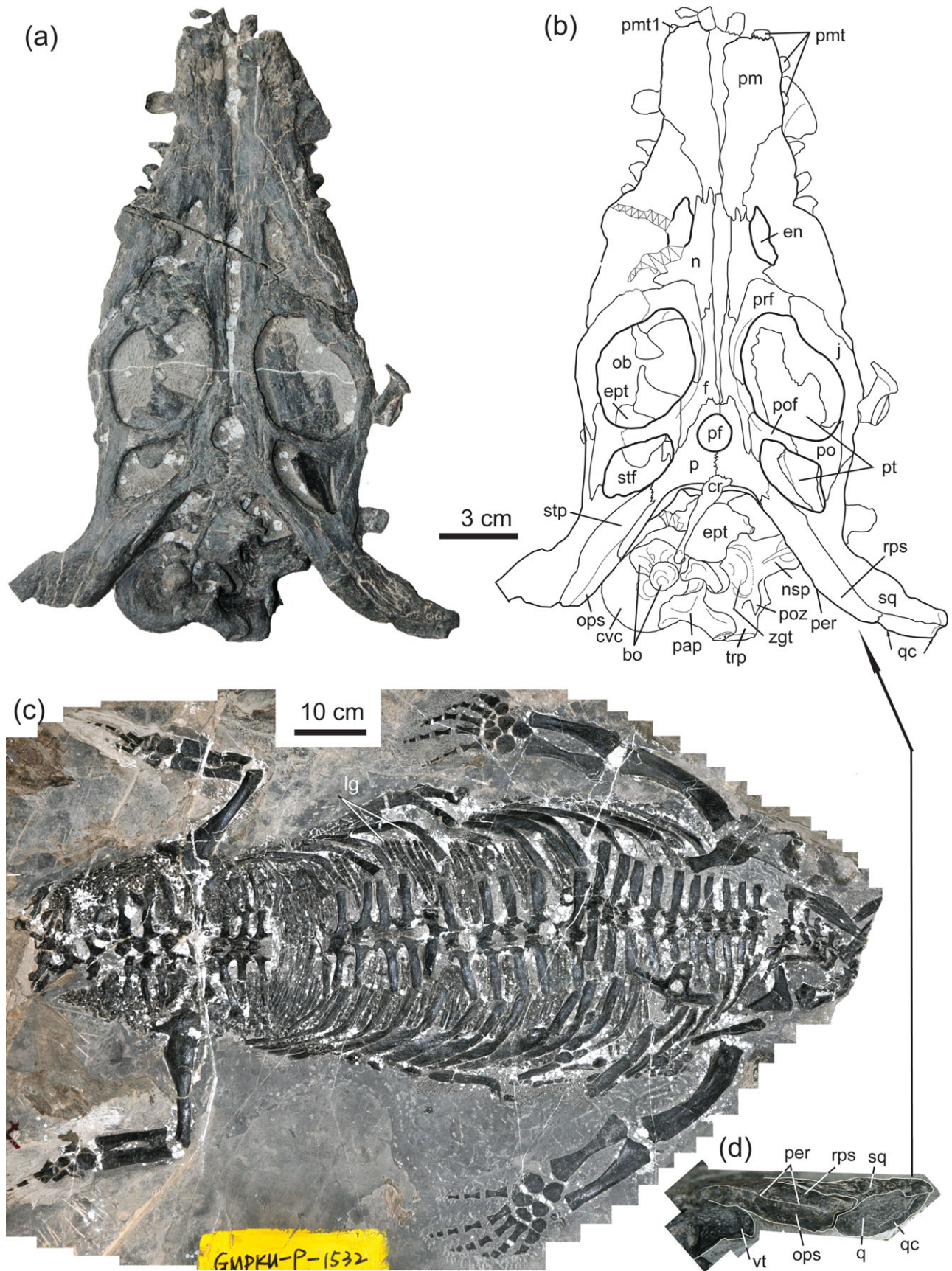


Figure 2. (Colour online) Referred specimens of *Largocephalosaurus qianensis* sp. nov. (a) Skull (GMPKU-P-1532-A) in dorsal view; (b) line drawing of (a); (c) skeleton (GMPKU-P-1532-B) in dorsal view; (d) right posterolateral portion of (a) in posterior and slightly dorsal view, interpretative lines have been added to highlight the structures of the relevant bones. Abbreviations as in Figure 1 plus: bo – basioccipital; cvc – centrum of an anterior cervical vertebra; cr – cervical rib; lg – lateral most gastral elements; nsp – neural spine; ob – orbital; ops – occipital portion of supratemporal; pap – paroccipital process; per – posterior edge of skull roof; pf – pineal foramen; pmt – premaxillary tooth; poz – postzygapophysis; qc – quadrate condyle; rps – roof portion of supratemporal; stf – supratemporal fenestra; trp – transverse process of vertebra; vt – vertebra; zgt – zygantrum.

Table 1. Selected measurements (in mm) of *Largocephalosaurus qianensis* sp. nov. from the type (IVPP V 15638), referred specimens GMPKU-P-1532-A (A) and GMPKU-P-1532-B (B)

Measurements	Type	A	B
<b>Skull</b>			
Midline length of skull (to occipital edge)	157	181	–
Length of snout	92	107	–
Maximum length of external naris	–	about 20 (R)	–
Maximum width of external naris	–	10 (R)	–
Length between naris and orbit	17 (L)	18 (L)	–
Maximum length of orbit	50 (L)	51 (L)	–
Maximum length of supratemporal fenestra	34.5 (L)	35.5 (R)	–
Maximum width of supratemporal fenestra	18.2	20 (L)	–
Length of parietal foramen	10	14	–
Width of parietal foramen	7.2	13	–
Length of suborbital fenestra	10 (L)	–	–
Width of suborbital fenestra	10	–	–
Width between external nares	19	21	–
Interorbital width	15	17	–
Intersupratemporal width	24	32	–
Length of retroarticular process	8	–	7.8
Width of retroarticular process	16	–	19
<b>Postcranial skeleton</b>			
Preserved length	2160	–	1279
Presacral length (without skull)	800	–	1175
Width of interclavicle	160	–	–
Midline length of interclavicle	46.5	–	–
Transverse width of clavicle	90	–	–
Total height of scapula	–	–	96
Maximum width of scapular base	–	–	51
Maximum width of coracoid	77	–	–
Minimum width	63	–	–
Humeral length	164	–	184(R)
Proximal width of humerus	39	–	37
Distal width of humerus	35	–	41
Length of ulna	118	–	121
Length of radius	110	–	133
Maximum width of pubis	64	–	–
Minimum width of pubis	49	–	–
Maximum width of ischium	79	–	–
Minimum width of ischium	45	–	–
Femoral length	136	–	155
Proximal width of femur	42	–	52
Distal width of femur	28	–	23
Length of tibia	82	–	102
Length of fibula	83	–	104
<b>Metacarpals</b>			
I	–	–	18
II	–	–	29
III	–	–	32
IV	–	–	36
V	–	–	27
<b>Metatarsals</b>			
I	15(L)	–	–
II	25(L)	–	–
III	–	–	27
IV	–	–	32
V	–	–	28
<b>Ventral length of vertebrae along ventral midline of centrum</b>			
3	12.5		
5	15		
10	19		
12	21		
21	28		
25	25		
31	27		
Sv1	26		
Sv2	27		
Cav1	26		
Cav5	25		
Cav8	25		
Cav15	24		
Cav20	22		

Cav – caudal vertebra; R – right; L – left; Sv – sacral vertebra.

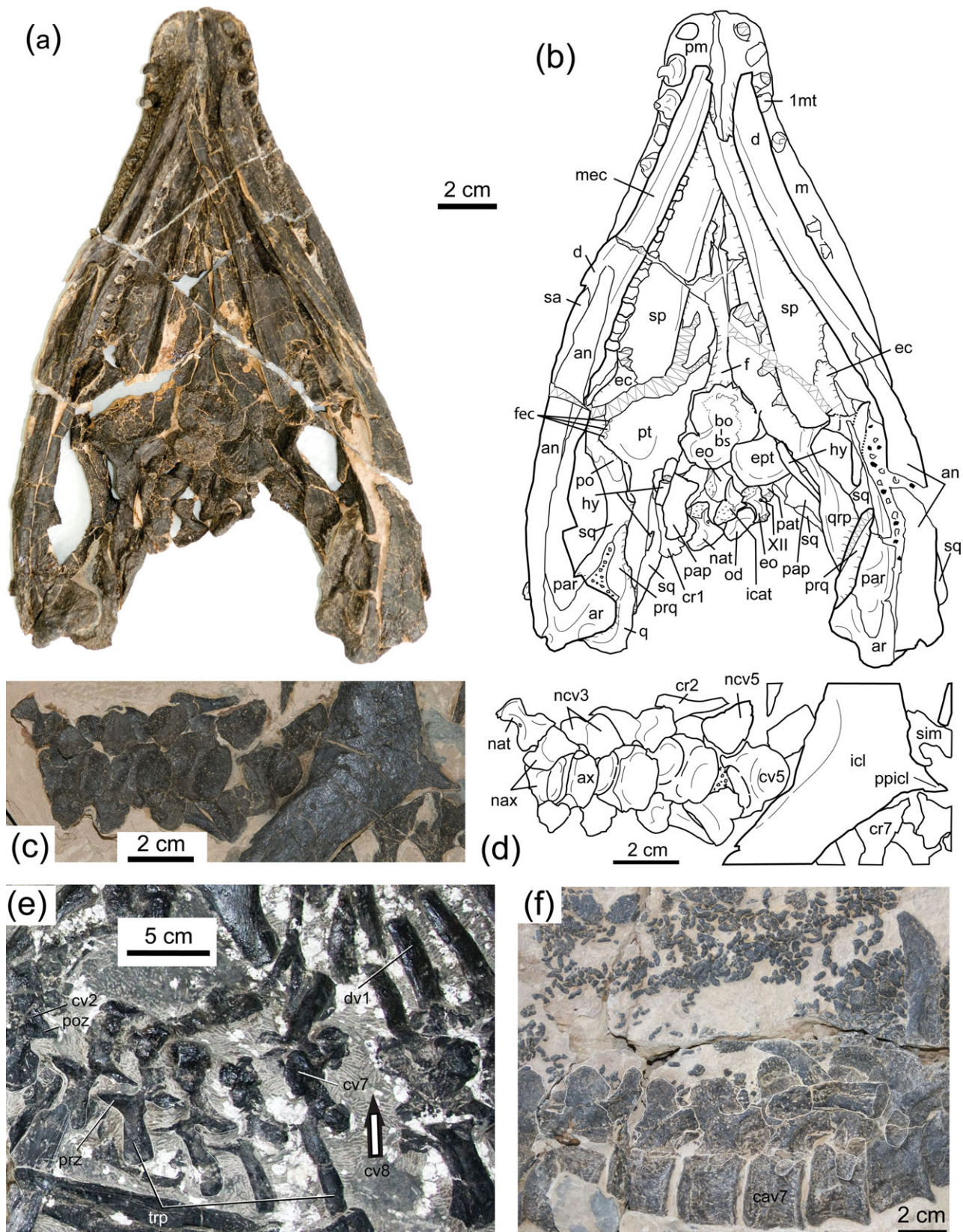


Figure 3. (Colour online) Skull and selected postcranial parts of *Largocephalosaurus qianensis* sp. nov. (a) to (d) and (f) type specimen (IVPP V 15638), (e) GMPKU-P-1532-B. (a) Skull in ventral view; (b) line drawing of (a); (c) most of cervical region in ventral view; (d) line drawing of (c); (e) cervical region in dorsal view, arrow indicating the displacement of cervical vertebra 8; (f) mid caudal vertebrae in right lateral and slightly ventral view, with many small, elongated granular osteoderms. Abbreviations as in Figures 1 and 2 plus: ar – articular; ax – axis; bs – basisphenoid; cav – caudal vertebra; cv – cervical vertebra; dv – dorsal vertebra; fec – facet for ectopterygoid; icat – intercentrum of atlas; icl – interclavicle; mec – Meckel’s canal; nax – neural arch of axis; ncv – neural arch of cervical vertebra; ppicl – posterior process of interclavicle; prq – pterygoid ramus of quadrate; prz – prezygapophysis; qrp – quadrate ramus of pterygoid; sq – splenial; 1mt – first maxillary tooth; XII – cranial nerve 12.

*Sinosaurophargis* (but see below). The dorsal surface of the parietal is weakly ridged and grooved.

The right maxilla of GMPKU-P-1532-A is nearly complete. It is large and forms a well-defined ascending process that extends dorsally posterior to the external naris and inserts a tip between the nasal and the prefrontal as in the type species (Fig. 2a, b). The maxilla sends a small anterodorsal process to meet the nasal and form the anterodorsal margin of the external naris posteriorly and meets the premaxilla anterodorsally. The lateral margin of the external naris is entirely formed by the maxilla. Along the margin of the upper jaw, the maxilla forms a slender, tooth-bearing posterior process that tapers to a tip at the level of the anterior three-fifths of the ventral margin of the orbit (Fig. 1b, c). The suture separating the ascending process of the maxilla from the prefrontal is simple. The tooth count of the maxilla cannot be established in either IVPP V 15638 (due to the occlusion of the mandible) or GMPKU-P-1532-A (where the dentition is not exposed). There are four and two teeth exposed *in situ* in the left and right maxillae of IVPP V 15638, respectively, and two and three teeth separately seen in the right and left maxillae of GMPKU-P-1532-A. The morphology of the maxillary teeth is the same as those of the premaxilla.

The complete prefrontal of GMPKU-P-1532-A is roughly hook-like in outline, with a short but broad anterolateral process forming the anterior margin of the orbit and a slender dorsal portion forming most of the dorsal edge of the orbit, contributing much more to the orbit than the frontal. As in other aquatic reptiles such as sauropterygians, no lacrimal foramen is present at the anterior margin of the orbit.

The nearly complete postfrontal and postorbital of GMPKU-P-1532-A are both triradiate in dorsal view (Fig. 2a, b). The former forms the granulated posterodorsal rim of the orbit anteriorly and the anteromedial margin of the supratemporal fenestra posteriorly. The dorsal surface of the postfrontal is heavily ornamented with ridges. The ornamentation of this bone is weak in IVPP V 15638 (Fig. 1b, c).

The postorbital is slightly larger than the postfrontal. Its descending ramus is shorter than the other two rami which form the major part of the bar between the orbit and the supratemporal fenestra and the supratemporal arcade, respectively. The postorbital–jugal contact is clear; the former articulates with the anterodorsal side of the latter. The postorbital–postfrontal suture is sharply curved while the postorbital–squamosal suture is strongly interdigitating, with a pointed posterior end of the postorbital inserting into the squamosal. The dorsal surface of the postorbital is weakly rugose. The relationships of the postorbital with the postfrontal and squamosal were obscured in the type species. The entrance of the squamosal to the orbit as described for the type species is questionable. Our examination suggests that the morphology of the postorbital in the type species is similar to that of the new species, with a large posterior (squamosal) process nearly forming the entire lateral edge of the supratemporal fenestra.

The jugal is well articulated with the neighbouring bones in GMPKU-P-1532-A; it is a simply curved, rod-like element, differing from the ‘boomerang’ shape of the bone in *Sinosaurophargis*. It forms the ventral border of the orbit anteriorly and tapers to a tip posterodorsally to insert between the postorbital and the squamosal as in *Sinosaurophargis*. Anteroventrally, the jugal sits on the posterior process of the maxilla. The lateral surface of the jugal is strongly convex along its length, with very light ornamentation. As with other skull bones, the morphology of the jugal is obscured owing to poor preservation; the sutures of the jugal with the maxilla and postorbital cannot be verified in the type species.

The squamosal is a large and irregular bone that was flattened during the process of fossilization. It is characterized by an elongate anterolateral process that meets the jugal to form the dorsal border of the ventrally opened infratemporal fenestra; in other words, the postorbital is excluded from the infratemporal fenestra as in *Sinosaurophargis*. The anterolateral process was described as entering the orbit in the type species, which was not supported by our examination. The parietal process is the smallest, forming the lateral fourth of the posterior border of the supratemporal fenestra. The ventral, or descending, process is huge and extends anteroventrally along the posterior border of the infratemporal fenestra, approaching the lateral side of the quadrate condyle (Figs 1b, c; 2a, b). The lateral surface of the squamosal is rough, with fine ridges and grooves.

The supratemporal is present, although its suture with the parietal is not always evident enough in all specimens including that of the type species. A strong line of evidence for the presence of this bone comes from its relationships with neighbouring elements. In reptiles, the parietal generally never meets the quadrate while the supratemporal, when it is present, always sits on the dorsal head of the quadrate medial to the squamosal; this relationship can be well exemplified in thalattosaurs (Nicholls, 1999; Wu *et al.* 2009). In the two skulls of the new species, the bone posteromedial to the squamosal clearly overlaps the dorsal surface of the quadrate shaft so that it cannot be referred to a large posterolateral process of the parietal but an independent supratemporal (Figs 1b, c; 2a, b). For the same reason, we argue that the supratemporal is also present in the type species as well as in *Sinosaurophargis*. The supratemporal appears as an elongate bone forming the lateral portion of the deep embayment-like posterior edge of the skull roof in dorsal view (Figs 1b, c; 2a, b). The supratemporal extensively covers the shaft of the quadrate but does not reach the quadrate condyle. Antero-medially, the bone enters the supratemporal fenestra. In posterior view, the supratemporal forms a strap-like occipital portion and extends distally along the posteromedial edge of the quadrate shaft (Fig. 2d).

The quadratojugal is most probably absent as in *Sinosaurophargis*. It cannot be traced in either IVPP V 15638 or GMPKU-P-1532-A.

The quadrate is largely covered by the squamosal and the supratemporal and dorsoventrally flattened. Its shaft is exposed only ventral to the supratemporal and posteroventral to the squamosal. The external surface of the shaft is not ornamented. The quadrate condyle is flattened and not so pronounced, the lateral half of the condyle must have been bigger than the medial half in life because of the different thicknesses. The medial/ventral surface of the shaft is notably concave. The lamina-shaped pterygoid ramus of the quadrate is visible in ventral view, and overlaps the lateral surface of the quadrate ramus of the pterygoid (Fig. 3a, b).

The palate can be observed only through the orbits in the type species but is exposed in ventral view in the type specimen of the new species. The edentulous palate is exposed between the two mandibular rami. Sutures between palatal elements are obscured in many places because of cracks. The pterygoid is a large, plate-like bone and separated from its counterpart along the midline anterior to the basisphenoid as in *Sinosaurophargis*. The palatine and vomer appear entirely covered by the displaced splenial and the symphyseal portion of the mandible. The interpterygoid vacuity is definitely present, probably with an elongate triangular shape (anteriorly narrow and posteriorly broad). Within the vacuity, the ventral surface of the frontal is exposed anterior to the basioccipital–basisphenoid complex (Fig. 3a, b). The central part of the pterygoid is broad

and articulates with the basiptyergoid process medially and meets the ectopterygoid and the palatine laterally; the latter is visible through the left orbit in dorsal view (Fig. 1b, c). The suborbital fenestra which is a common opening in diapsid reptiles is retained but was not confirmed in *Sinosauropsphargis*. The pterygoid contributes a small portion to the border of the suborbital fenestra. The large quadrate ramus of the pterygoid forms a deep blade-like lamina that is extensively overlapped laterally by the pterygoid ramus of the quadrate and, together with the latter, forms a nearly vertically oriented sheet to serve as the lateral wall of the middle ear chamber.

The palatine is visible through the orbits in dorsal view (Fig. 1b, c). It is broad, sheet-like and bears a shallow fossa on the dorsal surface. Our examination indicates that this fossa does not appear to be present in the type species. The bone forms the anteromedial half border of the oval suborbital fenestra.

The ectopterygoid is a small, disk-like element and exposed on both sides of the skull. Its maxillary suture is covered by the occluded mandible but its pterygoid suture is clear and visible in the left orbit in dorsal view. The ectopterygoid does not meet the palatine on the palate but it is unknown whether the two bones meet along the lateral border of the suborbital fenestra owing to the occlusion of the mandible. Both the ventral and dorsal surfaces of the bone are flat and smooth. The ectopterygoid was described as an anteroposteriorly elongate bone that sutures the palatine medially in *Sinosauropsphargis*. According to a further examination, the previously identified ectopterygoid is actually a jaw bone from the mandible, possibly the elongate coronoid. The true ectopterygoid is a broad, non-symmetrical rectangular bone, and largely overlapped by the pterygoid medially (see IVPP V 17040).

The epipterygoid is exposed in IVPP V 15638 and GMPKU-P-1532-A (Figs 1b, c; 2a, b; 3a, b). It is characterized by a broadened ventral portion and a peduncle-like dorsal shaft. The ventral portion is basally thickened and sits on a prominence on the dorsal surface of the pterygoid. The narrow dorsal shaft becomes thinner dorsally and bends slightly caudally. It may have contacted the ventral surface of the parietal just anterolateral to the prootic in life.

The braincase is exposed between the quadrate rami of the pterygoids (Fig. 3a, b). It is rather short and the basioccipital–basisphenoid suture is only partly identifiable. The basisphenoid projects into a pair of short, strong and anterolaterally directed basiptyergoid processes as in *Sinosauropsphargis*. The cultriform process appears very short if present. The basioccipital part forms a large, rounded occipital condyle and a fan-shaped anteroventral portion as shown in GMPKU-P-1532-A, although the latter was slightly damaged (Fig. 2a, b). A pair of foramina is present in the fan-like portion. Posterior to the occipital condyle, the two exoccipitals are exposed but disarticulated. The exoccipital and opisthotic are separate and preserved on both sides. The concave medial margin of the left exoccipital marks the contour of the foramen magnum on one side. The left exoccipital shows a small foramen that must have served for the exit of the hypoglossal nerve (Fig. 3a, b). The vagus (jugular) foramen, developmentally located between the exoccipital and opisthotic, is obscured due to the separation of the bones. The opisthotic is well exposed in GMPKU-P-1532-A (Fig. 2a, b), narrowing into a blunt tip distally as it forms the posterolaterally trending paroccipital process to contact the squamosal. The supraoccipital is exposed in dorsal view. It is more or less square in outline. A ridge, although very weak, is present along the midline. The external surface of the bone is slightly ornamented. The

left prootic is partly exposed in the supratemporal fenestra (Fig. 1b, c). It is posteriorly concave, which may mark the anterior border of the fenestra ovalis. Other features cannot be observed owing to the dorsoventral compression of the skull.

A rod-shaped element just posterior and slightly lateral to the prootic and medial to the quadrate ramus of the pterygoid on both sides is most probably the stapes (Fig. 1b, c). The proximal end of the stapes is thickened but slightly damaged, which has obscured the formation of a foot-plate in life. In ventral view, the stick-shaped hyoid is preserved on both sides (Fig. 3a, b), and the distal part of the right one can be also observed through the supratemporal fenestra medial to the stapes in dorsal view. The hyoid is proximally somewhat compressed, weakly grooved on its ventral surface and tapers distally.

The mandible cannot be entirely observed owing to the occlusion with the upper jaw in IVPP V 15638 (Figs 1, 3a, b); it is not preserved in GMPKU-P-1532-A and is fragmentary in GMPKU-P-1532-B (Fig. 4a). Two dentaries are split from each other and their anterior tips do not reach the first premaxillary teeth. This is also the case in *Sinosauropsphargis* and the type species (Li *et al.* 2011, fig. 2B; Cheng *et al.* 2012a, fig. 2), suggesting that the mandible may have been shorter than the upper jaw, or that the rostrum may have overhung the mandible to a certain degree in the Saurosphargidae in life. Anteriorly, the articular facets suggest that the symphysis of the dentaries is relatively long and stronger than in European pachypleurosaurs such as *Neusticosaurus* (Sander, 1989). Posteriorly, the dentary is deeply V-shaped to receive the surangular and angular. The disarticulation of the splenial exposed a deep Meckel's canal in the dentaries. The surface ornamentation of the dentaries is granular, with weakly-defined ridges. The dentary teeth are morphologically similar to those of the upper jaw. There is a series of 10 teeth exposed in the right dentary. The length of the portion with teeth missing suggests that there may have been five or more additional teeth. If so, there may have been at least 15 dentary teeth in total in life.

The disarticulated, sheet-like splenial extensively overlaps the palate. The anterior tip of the left splenial is complete and does not show an articular facet, suggesting that the bone did not meet its counterpart anteriorly and was not involved in the mandibular symphysis in life. The splenial is anteriorly narrow (dorsoventrally) and posteriorly broad; its posterior-most portion is missing. It is dorsally thin and ventro-medially thickened, and its labial surface is very concave to form the medial wall of the Meckel's canal.

The surangular is an elongate bone, more than the half length of the mandible. It is posteriorly thick and broad, extending posteriorly nearly to the end of the mandible where the bone terminated by a blunt end against the articular (Fig. 1b, c). Anteriorly, the surangular is narrow and tapers into a sharp process underlying the posterodorsal process of the dentary. Dorsally, the surangular shows a weak coronoid prominence, posterior to which the bone is concave. The external surface of the surangular (especially the posterior half) is smooth and lacking granules or ridges. The medial surface of the bone cannot be observed due to the displacement of the prearticular, and is poorly preserved in GMPKU-P-1532-B (Fig. 4a).

The nearly complete angular is even longer than the surangular, anteriorly reaching to the level of the fifth last dentary tooth of the dentition. As with the surangular, the angular has a broad posterior portion and narrow anterior portion. The former extends nearly to the end of the mandible and broadly covered the articular (Fig. 3a, b), and the latter terminates in a pointed end that inserts between the

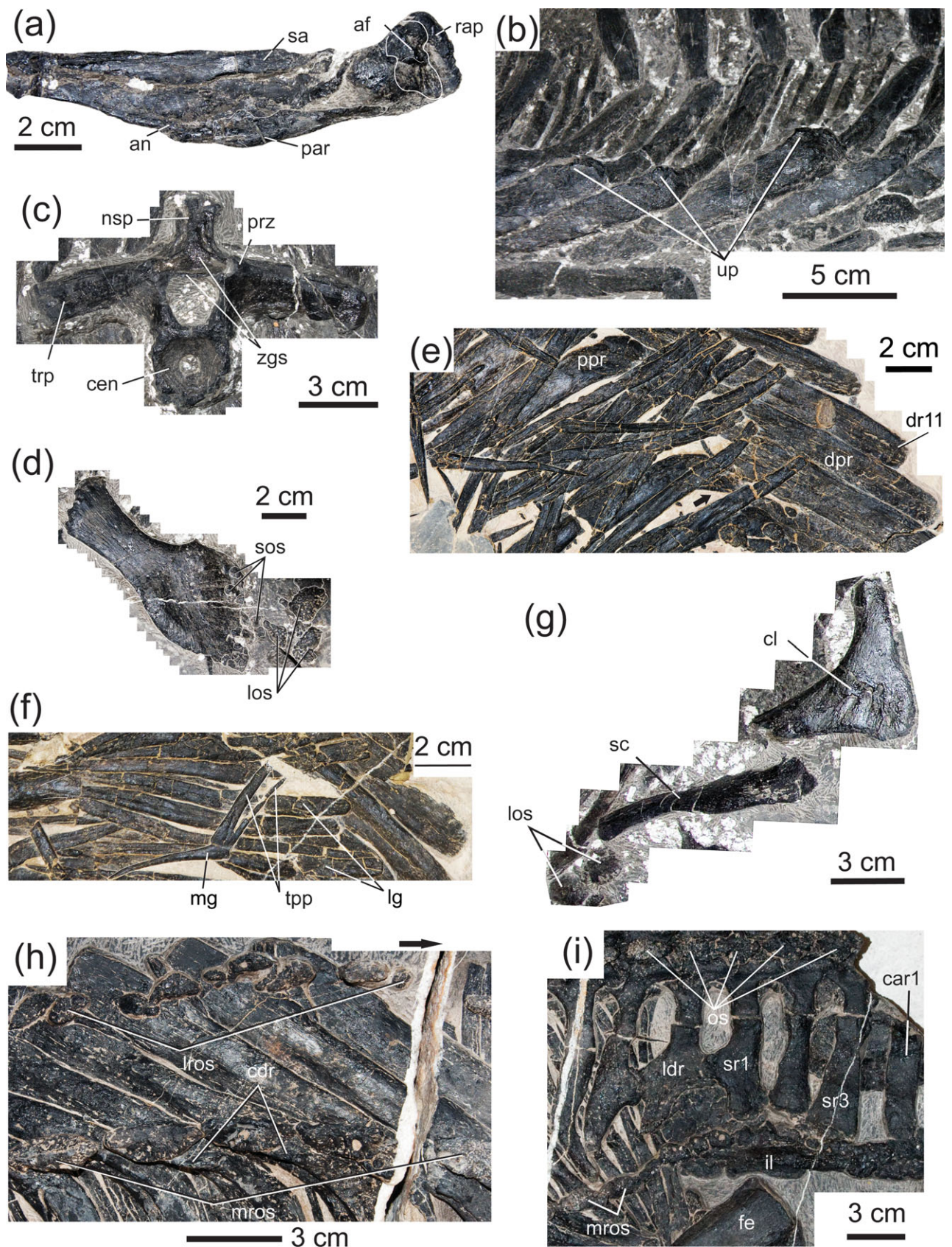


Figure 4. (Colour online) Various anatomical regions of *Largocephalosaurus*. (a) to (g) *L. qianensis* sp. nov.; (h) and (i) *L. polycarpon* (WIGM SPC V1009). (a) to (d) and (g) GMPKU-P-1532-B, (e) and (f) type specimen (IVPP V 15638). (a) Posterior portion of a right mandible in medial view, interpretative lines have been added to highlight the articular fossa; (b) lateral most portion of the right mid dorsal 'rib-basket' in dorsal view, showing the uncinata-like process of the dorsal ribs; (c) possibly the 8th cervical vertebra in anterior view, showing a single broad zygosphene; (d) left scapula in lateral view; (e) left mid dorsal 'rib-basket' in ventral view, showing a sharp rib angle (pointed by the arrow) between proximal and distal portions; (f) a disarticulated median gastral element with a two pronged lateral process on one side and the sheet-like structure formed by the lateral-most gastral elements; (g) right clavicle in anterolateral

dentary and splenial. The angular–surangular suture is more or less straight. The external surface of the angular is lightly granulated, forming weak longitudinal ridges.

The prearticular is another long bone although it is shorter than the surangular or angular. It is also posteriorly broad and anteriorly narrow (Fig. 3a, b). The bone forms the posteromedial half of the ventral side of the mandible and joins the formation of the medial wall of the adductor chamber. The prearticular–angular suture is slightly curved. The broad posterior portion narrows into a triangular process to overlap the angular. The narrow anterior portion tapers into a sharp end to contact the splenial. The smooth external surface of the prearticular is posteriorly concave and anteriorly convex.

The coronoid is elongate and located at the dorsal prominence of the surangular and extends anteromedially to meet the splenial anteriorly and the prearticular ventrally (Fig. 1b, c). Its anterior-most end is covered by the upper jaw. The occlusal surface of the coronoid appears granulated, with weak ridges along the dorsal length.

The articular is a stout element and transversely broadened for the articular fossa as seen in GMPKU-P-1532-B (Fig. 4a). In ventrolateral view, the bone is not entirely covered by the prearticular and angular, sending a sharp anterior process between the two bones (Fig. 3a, b). In ventromedial view, a ridge-like prominence extends antero-medially, resulting in a convex surface. Posteriorly, a short but broad retroarticular process is formed, which is thickened distally. In contrast, the retroarticular process of the type species is pronounced, with a sharply pointed end (Cheng *et al.* 2012a, fig. 2). In dorsal view, the articulated quadrate covers most of the articular, but the retroarticular process is visible, with a slightly concave dorsal surface. A foramen just posterior to the edge of the articular fossa may represent the foramen aërum.

#### 4.b. Vertebrae, ribs, gastralia and chevrons

**Vertebrae.** The vertebral column includes a section of 52 vertebrae from the atlas to the 52nd vertebra (in ventral view) and 23 posterior caudal vertebrae in two sections. The section of 52 vertebrae includes 9 cervical, 24 dorsal, 2 sacral, and 17 caudal vertebrae (Fig. 1a). The last cervical (the ninth) is distinguished from the first dorsal on the basis of the morphology of the rib attached; i.e. the rib is relatively short and slender, and tapers distally, while the first dorsal rib is clearly longer, more massive than the last cervical rib and distally thickened for the attachment of a cartilaginous segment presumably connected with the cartilaginous sternum ventromedially in life (Fig. 5a). In addition, the transverse process of the last cervical is also shorter and more slender than that of the first dorsal. The identification of the two sacral vertebrae was also based on the morphology of their ribs, or transverse processes, which are short but massive and bear a somewhat expanded distal end (Figs 5d, 6a). With the same criterion, three sacral vertebrae are recognized for the type species (Fig. 4i). The centrum of all vertebrae is deeply amphicoelous, as indicated by disarticulated vertebrae (Figs 2a, b; 3c, d; 4c).

The preserved part of the proatlas is hexagonal in outline, with a convex dorsal surface (Fig. 1b, c). The elements of the atlas are disarticulated. The nearly complete atlantal neural arches are still closely associated with the axial neural arch (Fig. 3c, d). The atlantal neural arches are medially very concave and laterally convex, showing an arc-like structure. Their base is thick and their spine portion is thin and antero-posteriorly expanded. It is difficult to know if the atlantal neural spine meets its counterpart of the other side. The atlantal intercentrum is wedge-shaped, anteriorly thick and posteriorly thin (Fig. 3a, b); it shows two facets for the articulation of the neural arch (anterolateral one) and the first cervical rib (posterolateral one).

The elements of the axis are largely articulated or closely associated (Fig. 3a–d). The stout odontoid process is partly wrapped by the atlantal intercentrum and an exoccipital anteriorly; the process bears a tongue-shaped projection anteriorly and a slightly convex posterior surface for the concave anterior surface of the axial centrum. The axial centrum is wider than long and shorter than that of cervical 3; it bears a facet for the neural arch. The axial neural arch is slightly displaced from the centrum, showing a part of the sutural facet with the centrum. The axial transverse process is invisible in IVPP V 15638 but exposed in GMPKU-P-1532-B, which is short and dorsoventrally broad (Fig. 3e).

A cervical vertebra attached to the occiput in GMPKU-P-1532-A is most probably a post-axial cervical on the basis of a short and strong transverse process for the rib and a stout neural spine (Fig. 2a, b). This vertebra is preserved in posterior view, showing a deeply concave surface of the centrum as in *Sinosaurosphargis*. The base of the neural arch just dorsal to the neural canal and medial to the postzygapophysis formed a broad and inclining surface that faces posteroventrally. The surface is nearly entirely occupied by a deep concavity (i.e. the zygantrium) which is not divided but well demarcated on both sides. The neural canal is not entirely exposed, and is nearly as wide as high in a disarticulated posterior cervical vertebra (Fig. 4c). The vertebra bears a broad but thin zygosphenes which is anteriorly incomplete. The aforementioned vertebrae and others do not show an evident pachyostosis in the zygapophyses or transverse processes. A fine preparation of WIGM SPC V 1009 indicates that the zygosphenes–zygantrium articulation is also present and the pachyostosis is absent too in the vertebrae of the type species.

The third to fifth cervical vertebrae are morphologically similar to each other in ventral view, with a short but broad centrum that is laterally constricted and lacks a ventral keel as in *Sinosaurosphargis* (Fig. 3c, d). As in the axis, the neural arch was not fused to the centrum in these cervicals and the sutural facet with the centrum is partly exposed owing to displacement. In dorsal view, the anterior cervical vertebrae of GMPKU-P-1532-B bear a relatively elongate transverse process when compared with those of *Sinosaurosphargis* (Fig. 3e). The transverse process is anteroposteriorly compressed, dorsoventrally broad and gradually becomes longer towards the dorsal vertebrae (Figs 2, 3e, 4c). The tip of the neural spine in those cervical

view and scapula in anterior view; (h) mid-portion of the left half of the trunk, showing two rows of osteoderms and dorsal crests of the trunk ribs in the type species; (i) left half of the sacral region, showing three sacral vertebrae and the connection of the last two dorsal ribs and the first sacral rib. Arrow in (e) and (h), indicates the turning angle and the head direction, respectively. Abbreviations as in Figures 1 to 3 plus: car – caudal rib; cdr – crest on dorsal surface of trunk ribs; cl – clavicle; cen – centrum of vertebra; dpr – distal portion of rib; dr – dorsal rib; fe – femur; il – ilium; ldr – the last dorsal rib; los – large osteoderms; lros – lateral row of osteoderms; mg – median gastral element; mros – medial row of osteoderms; os – osteoderm; ppr – proximal portion of rib; sc – scapula; sos – small osteoderms; sr – sacral rib; tpp – a two pronged lateral process of median gastral element on one side; up – uncinat process; zgs – zygosphenes.

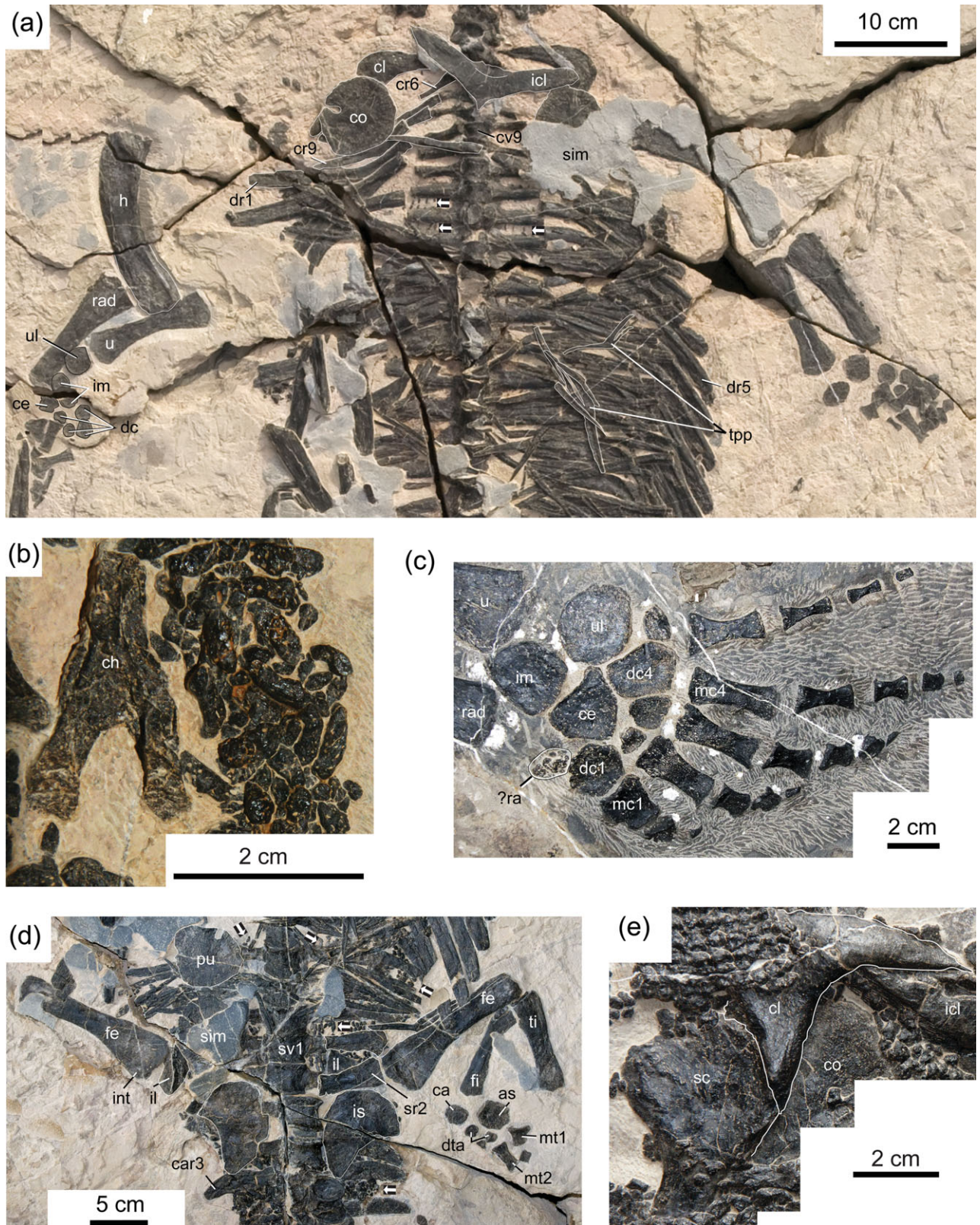


Figure 5. (Colour online) Girdles, limbs and caudal osteoderms of (a–d) *Largocephalosaurus qianensis* sp. nov. and (e) *Sinosaurosphargis yunguiensis*. (a), (b) and (d) IVPP V 15638 and (c) GMPKU-P-1532-B; arrows indicate dorsal lines or rows of small osteoderms in ventral view in (a) and (d); (a) anterior trunk in ventral view; (b) caudal osteoderms; (c) left manus in dorsal view; (d) sacral region in ventral view; (e) left side of the pectoral girdle of ZMNH M 8797 in dorsal view. Interpretative lines have been added to highlight the structures of relevant bones in (a), (d), (e). Abbreviations as in Figures 1 to 4 plus: as – astragalus; ca – calcaneum; ce – centrale; ch – chevron; co – coracoid; dc – distal carpal; dta – distal tarsal; fi – fibula; h – humerus; im – intermediate; int – internal trochanter; is – ischium; mc – metacarpal; mt – metatarsal; pu – pubis; ra – radiale; rad – radius; sv – sacral vertebra; ti – tibia; u – ulna; ul – ulnare.

vertebrae is somewhat broad, forming a table-like plate that becomes further broadened posteriorly. Cervical vertebrae 6 to 8 are mostly covered by the interclavicle in IVPP V 15638 but are exposed dorsally in GMPKU-P-1532-B (Fig. 3e). As in the anterior cervicals, the transverse process gets longer and the dorsal table of the neural spine becomes broader toward the dorsal series. These two structures of cervical 9 are similar to those of the first dorsal but the transverse process is just shorter and more slender than that of the latter. Both pre- and postzygapophyses in all cervicals except for the atlas are well-developed and positioned at nearly the same level; their articular facets appear more vertical than horizontal in orientation.

The 24 dorsal vertebrae are exposed in ventral view in IVPP V 15638 and in dorsal view in GMPKU-P-1532-B (Figs 1a, 2c). The centrum is slightly laterally compressed and, like the cervical series, lacks any ventral keel; it gets longer towards the mid dorsals and then shortens towards the sacrum. The neural spine is as low as that of the last two cervicals, the transverse process gets longer gradually until dorsal 9 and then changes little in length to dorsal 15. Thereafter, the transverse process shortens posteriorly, and those of the last dorsal are just slightly longer than that of the sacral vertebrae. Compared with those of *Saurosphargis* and *Sinosauropsphargis*, the transverse process of the dorsal vertebrae is more slender, not much wider than the space between the adjacent processes. In all dorsals, the top table of the neural spine is well-developed, reaching the greatest degree in the mid dorsals. Well-developed pre- and postzygapophyses are very similar to those of the posterior cervicals in position and orientation. It is evident that the neural arch is not fused to the centrum in those dorsals exposed in lateral view.

The two sacral vertebrae have shorter and more massive transverse processes and a broader top table of the neural spine when compared with the posterior dorsals. As shown in the preserved caudal vertebrae, the neural arches are still not fused to the centra (Fig. 3f), suggesting that IVPP V 15638 was not an old adult. In GMPKU-P-1532-B, the preserved anterior caudals (the first four) are similar to the sacral and posterior dorsals in that the neural spine is narrow and its top table is still evident and covered by osteoderms (Fig. 6a); the top table narrows in the fifth caudal and disappears in the further posterior caudals in IVPP V 15638 (Fig. 3f). From the fifth backwards, the neural spine is relatively taller than in the sacral and posterior dorsal vertebrae, with a convex dorsal margin. The centrum is as broad as high in anterior caudals and becomes longer than high in posterior caudals, in which the neural spine becomes very low.

**Ribs.** A slender element mixed with skull bones on the right side in IVPP V 15638 was identified as an atlantal rib (Fig. 3a, b). It was displaced, with its thickened single articular head facing posteriorly and its slender shaft pointing anteriorly. The axial rib also appears to be single-headed, with a narrowed distal portion (Fig. 3c, d). The visible cervical rib 7 and further posterior ribs are all single-headed; as such, all cervical ribs are most probably single-headed and distally narrowed. Cervical ribs become longer towards the dorsal series. The first dorsal rib from vertebra 10 is much thicker and longer, with a blunt distal end for a cartilaginous segment to connect with the pectoral girdle, as mentioned earlier. As shown in GMPKU-P-1532-B (Fig. 2c), the dorsal ribs bear an uncinat-like process along the curved posterior margin of the shoulder region. In detail, this uncinat process is not as pronounced as in *Saurosphargis* but is much more laterally expanded (Figs 2c, 4b). The uncinat process of *Eusauropsphargis* is very different; it

is very narrow, extremely pronounced and projecting from the convex margin of the shoulder region of dorsal ribs. No uncinat process is present in *Sinosauropsphargis*. Further preparation of WIGM SPC V 1009 revealed that the type species of *Largocephalosaurus* does not have such an uncinat process in dorsal ribs but a strong crest on the external (dorsal) surface of the shoulder region of the dorsal ribs (Fig. 4h). As in the other saurosphargids, the lateral portions of the dorsal ribs are broadened to abut each other, forming a 'rib-basket'. The proximal portion of the dorsal ribs is relatively narrow when compared to that of *Saurosphargis* and *Sinosauropsphargis*, matching the slender transverse process of the dorsal vertebrae as in the type species. The turning angle at the shoulder of the dorsal ribs is evidently smaller than that in *Saurosphargis* and *Sinosauropsphargis*, suggesting a body shape that is a more elongated oval than that of the latter two (Figs 1a, 2c, 4b, e). The last three or four dorsal ribs are slender and short, with a pointed distal end not joining the formation of the 'rib basket'. The two sacral ribs are shorter than the last dorsal but much more robust, with a slightly expanded and slightly thickened distal end (Figs 5d, 6a). In contrast, the last two dorsal ribs and the first sacral rib are connected together by processes in the type species (Fig. 4i), which is unique within the Triassic aquatic reptiles. All caudal ribs are not fused with the caudal vertebrae; the anterior caudal ribs are longer than the sacral ribs. All caudal ribs taper off distally and curve posteriorly, become shorter and shorter posteriorly and disappearing probably at the 10th or 11th caudal vertebra.

**Chevrons.** Displaced chevrons are stick-shaped in lateral view, with a slightly expanded proximal and a distal end (Fig. 1a). They are of the typical Y-shape in anterior or posterior view, with the forked proximal portion evidently shorter than the distal symphysis (Fig. 5b).

**Gastralia.** Gastral ribs are disarticulated and scattered in IVPP V 15638 and partly visible in dorsal view in GMPKU-P-1532-B (Figs 1a, 2c). As in *Sinosauropsphargis*, the lateral-most segments broaden to form a sheet-like structure and the angulated median segment does not form an evident anterior knob or process but often has a two-pronged lateral process on one side (Figs 4f, 5a). Such a lateral process of the median gastral segment was not described for *Sinosauropsphargis* (Li *et al.* 2011). Our examination of the specimens found that a scattered median gastral segment of the paratype (IVPP V 16076) clearly bears a two pronged lateral process on one side, which was also shown in a photo of the specimen in Li *et al.* (2011, fig. 3B). Such a median gastral segment was also present in *Saurosphargis* and *Eusauropsphargis* (Nosotti & Rieppel, 2003), *Sinosaurus* and *Nothosaurus* (Rieppel, 1998b) and *Corosaurus* (Storrs, 1991, fig. 10H, I). It was not reported in *Hanosaurus* (Rieppel, 1998a) but a photo (Rieppel, 1998a, fig. 3C) clearly shows that one or two median gastral segments had a two-pronged lateral process on one side. Our examination of the type specimen IVPP V 3231 further confirmed the presence of such a median segment in *Hanosaurus*.

#### 4.c. Osteoderms

Osteoderms are present on the dorsal surface of the body but they do not form a carapace to completely cover the trunk, as was described for *Sinosauropsphargis*. They consist of many small, elongated granular elements that are arranged in lines or rows on the dorsal surface of the trunk and assembled together as a sheet to cover the lateral side of

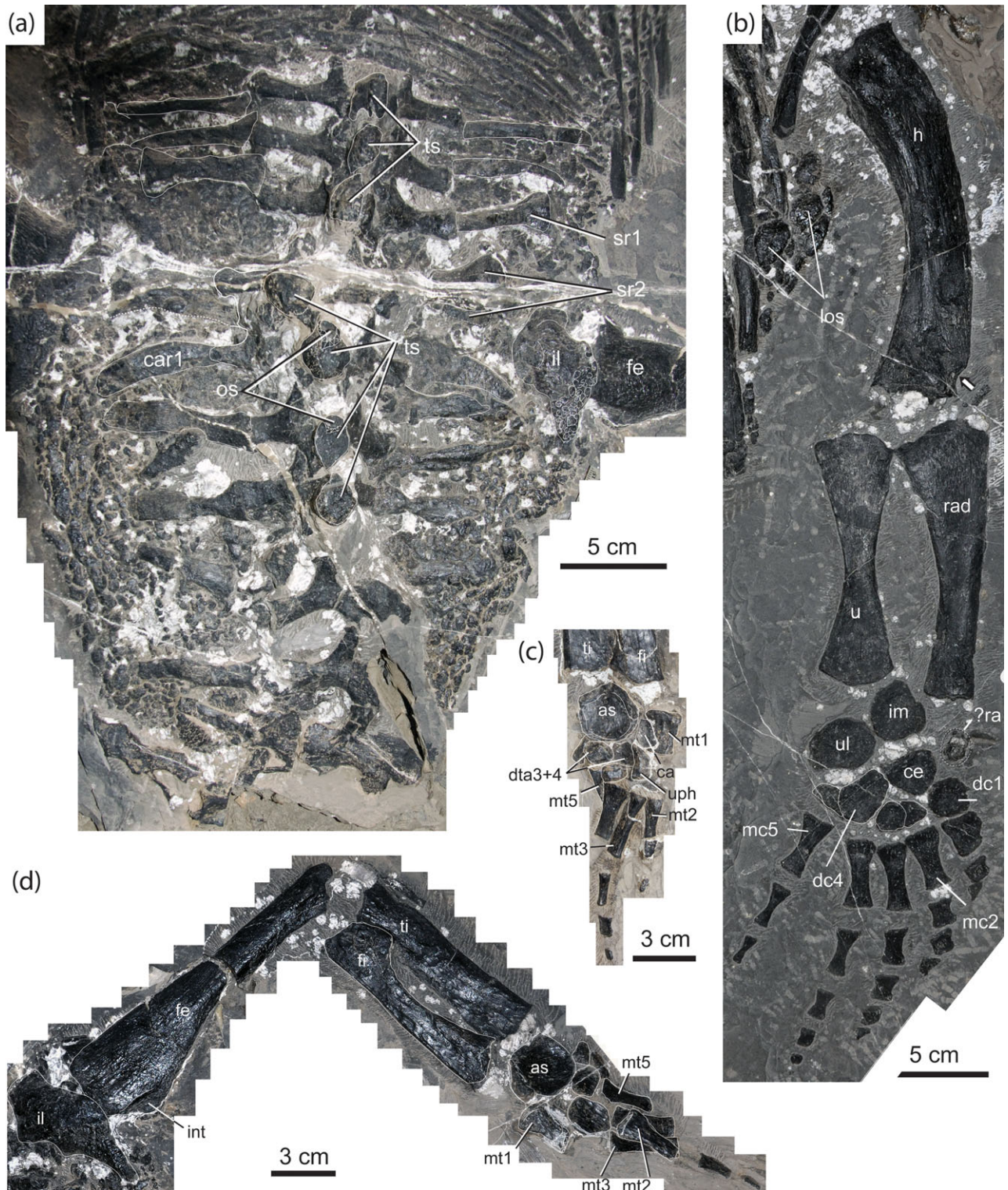


Figure 6. (Colour online) Pelvic girdle and limbs of *Largocephalosaurus qianensis* sp. nov. in dorsal view (GMPKU-P-1532-B). (a) Sacral region, showing large and small osteoderms; (b) right forelimb; (c) left pes; (d) right hindlimb. Interpretative lines have been added to highlight the structures of relevant bones. Arrow in (b) indicates the ectepicondylar notch. Abbreviations as in Figures 4 and 5 plus: ts – dorsal table of neural spine; uph – ungual phalanx.

the body, especially in the regions close to the pelvis and along the side of the tail where they are mixed with some large elements (Figs 3f, 5b, d, 6a). In addition, there is a median row of large elements running along the dorsal tables of the neural spines although the osteoderms of this row are poorly preserved and appear not always to contact each other (Fig. 2c). The dorsal rows of small osteoderms seen

in IVPP V 15638 (Fig. 5a) are widely separate from each other. These rows of small osteoderms were not preserved in GMPKU-P-1532-B, where they may have been cleaned out during preparation. The osteoderms of the median row are well-preserved in the neck region and sacral region in the type species, showing an elongate oval contour. The osteoderms meet each other at both ends and have a one to

one relationship with the vertebrae; each osteoderm covers one half of the dorsal table of each of the two neighbouring neural spines (Fig. 4i). This indicates that the new species may have had a similar median row of osteoderms in life. There is no evidence of osteoderms on the ventral surface but something like 'skin impression' in IVPP V 15638, some of which was intentionally not removed during preparation (Figs 1a, 5a, d). The 'impression' has no evident structure but is in lightly greenish colour and restricted to the ventral surface of the body. We have no convincing evidence to support the suggestion that the coloured patches represent the impression of the true skin of the animal.

Osteoderms are also present on the dorsolateral surface of the body in the type species, as shown in the partly prepared trunk region (Fig. 4h). They differ from those of the new species in that they are much larger and regularly arranged, forming two longitudinal rows separately along the lateral side of the trunk region. The medial row runs along the aforementioned crests on the rib shoulders and the lateral row runs along the lateral-most side of the trunk (Fig. 4h). The osteoderms of the medial row are large and connected to one another, while those of the lateral row are small and massed together along the body side. The two rows of the osteoderms finally converge together when they reach the pelvis.

#### 4.d. Pectoral girdle

Each element of the pectoral girdle is well represented in IVPP V 15638 or GMPKU-P-1532-B. The scapula is not significantly different from that of the type species, with a stout dorsal blade and a broadened base (Fig. 4d, g). The dorsal blade is slightly constricted and distally truncated, and the ventral base is laterally concave, with a weak prominence, the acromion, along the anterodorsal margin. The glenoid surface is nearly vertical to the articular facet for the coracoid and also nearly parallel to the acromion in orientation. Compared with that of other marine reptiles, the scapula is most similar to that of *Corosaurus*, an eosauroptrygian in which the distal end of the dorsal blade is relatively more expanded (Storrs, 1991, fig. 12A, B).

The coracoid was displaced; it is simply a round plate with an open coracoid foramen. The foramen was probably bordered by the articulation of the scapula in life (Figs 1a, 5a). The nearly circular outline differs from that of any other Triassic marine reptiles including *Eusaurosphargis* in which the coracoid is roughly a rectangular or bilaterally constricted bone with an open coracoid foramen. No coracoid was exposed in *Sinosaurosphargis*. The semi-oval outline of a partly exposed bone on the ventral surface of the only specimen of *Saurosphargis* appears comparable to a coracoid in size and shape (Nosotti & Rieppel, 2003, fig. 11). If so, it is more similar to the coracoid of *Eusaurosphargis* than the coracoid of the new species here. The roughly round coracoid of *Helveticosaurus* from the Middle Triassic of Europe is the most similar in outline although its open coracoid foramen does not reach so deeply into the bone (Rieppel, 1989, fig. 6).

The clavicle differs little from that of the type species, showing an angulated outline. Its two arms enclose an angle of about 90° and are distally pinched off (Figs 4g, 5a). As shown in GMPKU-P-1532-B, the clavicle articulates with the dorsomedial side of the scapula (Figs 2c, 4g). In lateral view, the surface of the bone is rough, with fine ridges or striations. Its internal surface is not exposed. Compared with that of *Sinosaurosphargis*, the anterolateral corner of the clavicle is rounder. The clavicle was described as articulating with the dorsolateral side of the scapula in *Sinosaurosphargis* (Li

*et al.* 2011). Our further examination of a referred specimen (ZMNH M 8797) of this taxon did not support this view, but revealed the same pattern of articulation as in the new species (Fig. 5e).

The interclavicle is well exposed and shows an intermediate outline between a typical T-shape and boomerang-shape in ventral view (Figs 1a, 3c, d, 5a). Its anterior margin is very concave and its posterior 'shaft' is very short and sharply pointed. Its external surface is slightly convex, with fine striations laterally and its internal surface is not exposed. In detail, the interclavicle differs from that of *Sinosaurosphargis*. In the latter, the bone is relatively broad, more triangular in outline (see ZMNH M 8797); its anterior margin is slightly concave and its two posterolateral margins are nearly straight.

#### 4.e. Forelimbs

The forelimbs are well-preserved in dorsal view in GMPKU-P-1532-B (Fig. 2c) and partly preserved in ventral view in IVPP V 15638 (Figs 1a, 5a). The humerus resembles that of the type species and is similar to that described for *Sinosaurosphargis* (Li *et al.* 2011), with a shaft strongly curved posteriorly, convex anteriorly and slightly concave ventrally. Both proximal and distal portions of the humerus are slightly expanded but it appears slightly constricted near the proximal and distal extremities and has no epiphysis-like structure to form a prominent articular head proximally or condyle distally. No ectepi- and entepicondylar foramina are present but an ectepicondylar groove is evident and anteriorly notched (Fig. 6b). In contrast, the entepicondylar foramen is present in the type species (Cheng *et al.* 2012a, fig. 3).

Both the radius and ulna are, again, very similar to those of the type species and also comparable to those of *Sinosaurosphargis*. They are laterally convex and medially concave (Figs 5a, 6b). The radius is slightly longer than the ulna (Table 1). The former is proximally expanded, with an articular surface asymmetrically convex, and distally narrow, with a flat surface for the carpals. The ulnar side of the bone is concave and its lateral side is straight. The ulna is similarly expanded at both the proximal and distal ends and its articular facets for the humerus and carpals are convex.

There are nine carpals preserved in GMPKU-P-1532-B (Figs 2c, 5c, 6b). The ulnare and intermedium distal to the ulna are similar in size, both with an atypical circular outline. The former bears a convex surface for the ulna and slightly concave surface for distal carpals; the latter also has a convex surface for the ulna and a curved surface facing the radius. The triangular carpal between the intermedium and distal carpals 2 and 3 was identified as a centrale, which is smaller than the aforementioned two carpals. The distal carpal series consists of five elements, with the fourth one being the largest and then the first one; the second is the smallest and the other two are similar in size. The fourth carpal is more or less rectangular, the first is nearly circular and the others are irregular in outline. There is a small bone, similar to distal carpals 2 or 5 in size, between the radius and distal carpal 1 in both forelimbs although it is closer to the distal carpal 1 and the central than to the radius in the left manus. We assume that this bone is most probably the radiale as in the type species and the latest to fully ossify among all carpals in the individual. In *Sinosaurosphargis* (Li *et al.* 2011, fig. 1B), there is also a small bone between the radius and distal carpal 1 and it is similar to distal carpals 4 and 5 (the latter was not counted as one in Li *et al.* 2011) in size. If it is considered as the radiale then the manus of *Sinosaurosphargis* had the same number of

carpals as described here. The presence of eleven carpals is the most peculiar feature of the type species (Cheng *et al.* 2012a, fig. 3). If the pisiform and distal carpal 5 elements described by Cheng *et al.* (2012a) are not counted and some of the others are renamed, the number and arrangement of the carpals are essentially identical in the type and new species. As arranged in GMPKU-P-1532-B, the type centrale 3 should be distal carpal 4; distal carpal 4 should be distal carpal 5; and centrale 2 is the only centrale as described here. Our further examination indicates that the pisiform and carpal 5 elements described by Cheng *et al.* (2012a) in the type species, are actually three elements. Do these three elements represent three displaced osteoderms or extra ossifications of the carpus? The surface morphology is similar to that of other carpals, favouring the latter explanation. Unfortunately, the manus of the other side was not preserved and more specimens are therefore needed to verify whether the carpus of the type species had extra ossifications.

The five metacarpals do not overlap each other at their base as in *Sinosaurophargis* (Figs 5c, 6b), suggesting an expanding pattern of the manual fingers in saurophargids. The fourth metacarpal is the longest, slightly longer than the third and then followed by the second and the fifth. The first metacarpal is the shortest, evidently shorter than the second, but the most robust. In thickness, the other four are similar. The aforementioned metacarpal features are also true in *Sinosaurophargis*; the only visible difference is that the first metacarpal is relatively less massive in the latter. As for the phalangeal formula, the pattern of 2–3–4 for the first three fingers is convincing because they are terminated by an unguis phalanx in both forelimbs. The fourth finger has four phalanges preserved, of which the fourth phalanx is much shorter than the others as is the penultimate phalanx of the type species; with the addition of the unguis phalanx, the fourth finger should have had five phalanges in life. Among the preserved three phalanges of the fifth finger, the third one is still much longer than wide as in the type species; in the latter, the fourth phalanx of the finger is small and square in outline and followed by the terminal unguis phalanx. If it is also true for the new species, then the fifth finger may have had five phalanges and the phalangeal formula of the manus may have been of 2–3–4–5–5 as in the type species.

#### 4.f. Pelvic girdle

Three elements of the pelvic girdle are well-exposed in IVPP V 15638 and GMPKU-P-1532-B. The right ilium of the latter is exposed mainly in dorsal and slightly medial view (Fig. 6a, d). It has a low dorsal blade with a convex dorsal edge and an evident process directed posteriorly and slightly dorsally, and being distally pinched into a pointed end. Medially, the bone surface is very convex but no articular facet can be traced owing to many small covering osteoderms. For the type species, further preparation clarified the morphology of the ilium which differs little from that of the new species; there is a crest projecting above the acetabulum, but this region is not exposed in the new species. The ilium of the Middle Triassic *Sanchiaosaurus* appears similar in outline (Rieppel, 1999, fig. H).

The pubis is almost a round plate as in type species and its nearly circular outline is also similar to the coracoid although slightly smaller in size (Figs 1a, 5d). Its obturator foramen is open and its sutural margin with the ischium is thickened. Among the Triassic marine reptiles from China, the round pubis of *Hanosaurus* is most comparable, nearly identical in morphology (IVPP V3231; Rieppel, 1998a, fig. 5).

The ischium is kidney-like but asymmetrical in outline, with a large proximal/lateral portion and a narrow

distal/medial portion; in other words, the bone is antero-medially convex and posterolaterally concave (Fig. 5d). In morphology, the ischium is again most comparable to that of *Hanosaurus* if the evidently concave margin between the iliac and pubic facets illustrated in Rieppel (1998a) is not considered. Our examination of the *Hanosaurus* specimen IVPP V 3231 reveals that there is actually no such concave margin but a tiny shallow notch in its place (also see Rieppel, 1998a, fig. 1b). As with the pubis, the sutural margins are thickened and facets for the ilium and pubis are not evidently separated.

#### 4.g. Hindlimbs

Elements of the hindlimbs are well-preserved except for those of the autopodium; they are exposed in ventral view in IVPP V 15638 but in dorsal view in GMPKU-P-1532-B (Figs 1a; 5d; 6c, d). The femur morphologically resembles that of the type species, having a straight shaft with a strongly expanded proximal head and a slightly broadened distal portion. Its anterolateral margin is straight but its posteromedial edge is concave. Anterolaterally (extensor aspect), the shaft surface is very convex, with an elongate prominence along the bone length. The internal trochanter is developed and proximally positioned as in *Corosaurus* but not *Hanosaurus* where it is located far from the proximal end. As shown in IVPP V 15638, an intertrochanteric fossa is very shallow but evident. Distally, no evident tibial condyle is formed and the end is not broadened, a condition which is different from the well-expanded distal end seen in *Eusaurophargis* (Nosotti & Rieppel, 2003, fig. 18). Posteriorly/medially, the shaft surface is somewhat concave.

The fibula and tibia are in articulation in GMPKU-P-1532-B and basically similar in morphology to those of the type species (Fig. 6d). The two ends of the fibula are expanded. The proximal surface is asymmetrically convex with a facet for the femur and a facet for the tibia, and the distal surface is slightly convex for the astragalus. It is very concave along the tibial side and nearly straight along the lateral side. The tibia is column-shaped, with no expansion at both ends. This is not the case in the type species where the proximal end is evidently broader than the distal end and the fibular margin is concave. Both the proximal and distal surfaces of the tibia are slightly concave.

There are four tarsals, consisting of the astragalus, calcaneum and two distal tarsals (Figs 5d, 6d). The astragalus is the largest element and disk-like in outline; its facets for the fibula and tibia are slightly concave, and its posterior surface is concave. The calcaneum is complete in IVPP V 15638, smaller than the astragalus but larger than the two distal tarsals; it is nearly oval and structurally simple. The two distal tarsals are identified as distal tarsals 3 and 4, as in the type species.

The five metatarsals are better preserved in GMPKU-P-1532-B than in IVPP V 15638 although they are not in articulation. Metatarsal 1 is the most massive and shortest, with a base being widest among the metatarsals (Fig. 5d). Metatarsal 5 is slenderest, shorter than metatarsals 2 to 4. Metatarsals 2 and 4 are similar in length but the former is more slender than the latter (Fig. 6c, d). Metatarsal 3 is the longest and its shaft is thicker than metatarsal 2 but thinner than metatarsal 4. The shaft of all metatarsals is bilaterally somewhat constricted. In contrast, metatarsal 4 is the longest and also the slenderest among metatarsals in the type species. Furthermore, metatarsal 5 is second in thickness and as long as metatarsal 3 in the type species. According to our observation of WIGM SPC V 1009, metatarsal 5 of the type

species is also unique in that it bears a projection at the lateral margin, just proximal to the distal end.

Pedal phalanges are not in articulation and poorly preserved in both type and GMPKU-P-1532-B, and the pedal phalangeal formula cannot be restored. Among the preserved phalanges, an unguis phalanx is present in GMPKU-P-1532-B, which is laterally compressed and its ventral side is not strongly curved.

## 5. Phylogenetic relationships

*Largocephalosaurus* was originally considered to be a sauropterygian, phylogenetically nested in a clade including typical pachypleurosaurs and nothosaurs (Cheng *et al.* 2012a). This result was based mainly on skull characters because the postcranial skeleton was not then available for study, and details of the well-preserved saurosphargid *Sinosaurosphargis*, had not yet been published for comparison. With the discovery of the new species, many anatomical features such as the close 'rib-basket', the lateral gastral elements forming a sheet-like structure, the deeply 'V'-shaped posterior edge of the skull roof, the retention of the interpterygoid vacuity, the peculiar tooth morphology and well-retracted external naris strongly suggest that *Largocephalosaurus* is not a sauropterygian but may have had a close affinity to the Saurosphargidae. On the other hand, the phylogenetic relationship of the Saurosphargidae was hypothesized to be close to thalattosaurs (Li *et al.* 2011), which differed from Nosotti & Rieppel (2003). For testing those competing hypotheses, we reanalysed the phylogenetic relationships based on a data matrix derived from that of Li *et al.* (2011). The derived data matrix included the addition of *Largocephalosaurus* and a Chinese pistosaur *Yunguisaurus* (Cheng *et al.* 2006; Sato *et al.* 2010), two new characters, the modification of some characters and character state coding changes in some taxa (see Table 2). In the current analysis, the new and type species of *Largocephalosaurus* are treated as two separate terminal taxa; for the type species, the character state coding is based on the skull as well as the newly prepared postcranial skeleton. The current data matrix consists of 39 terminal taxa (including the Ichthyopterygia) and 159 characters.

In our reanalysis, using PAUP 4.0b10 (Swofford, 2002), the resultant trees were rooted on an all-0-ancestor. An heuristic search with all characters equally weighted and all multistate characters unordered yielded 11 most parsimonious trees, each with a tree length of 570 steps, a consistency index of 0.3842, and a retention index of 0.6710. Interrelationships among the clades of the various marine reptiles included (i.e. Sauropterygia, Saurosphargidae, *Helveticosaurus*–*Eusaurosphargis* clade, Thalattosauria and Ichthyopterygia) are well established but not for other groups in the strict consensus of 11 most parsimonious trees (Fig. 7a). In contrast to Li *et al.* (2011), the Saurosphargidae is the sister-group of the Sauropterygia rather than the Thalattosauria

although this relationship is not further supported by the bootstrap search owing to a low value for the monophyly of the latter, as found by Li *et al.* (2011). This result also differs from Nosotti & Rieppel (2003) in which thalattosaurs formed the sister-group of the Sauropterygia. For other marine reptilian groups, the *Helveticosaurus*–*Eusaurosphargis* clade, thalattosaurs and Ichthyopterygia form a set of successive sister-group relationships toward the Saurosphargidae–Sauropterygia clade, which also differs from Li *et al.* (2011) who found that interrelationships among all included marine reptilian groups entirely collapsed when the Ichthyopterygia was included in their analysis (see Li *et al.* 2011, fig. S1). Bootstrap support is 63 % for the monophyly of a clade including all aforementioned marine reptilian groups; 100 % for the monophyletic Saurosphargidae; 61 % for *Saurosphargis*–*Sinosaurosphargis* sister-group relationship; and 65 % for the sister-group relationship of the two species of *Largocephalosaurus* within the family. Monophyly of the Sauropterygia was not supported in the bootstrap analysis, and their relationships with the *Helveticosaurus*–*Eusaurosphargis* clade, thalattosaurs and Ichthyopterygia were not resolved. As Li *et al.* (2011) suggested, these low support values may have been the result of the large amount of missing data for *Helveticosaurus* and *Eusaurosphargis*, the extreme specialization of the Ichthyopterygia and a large amount of convergence amongst the taxa included in the analysis. To test the interference of the Ichthyopterygia, we did the second analysis with the group excluded and an identical setting of the data matrix as in the first analysis. This analysis produced 16 most parsimonious trees, each with a tree length of 546 steps, a consistency index of 0.4011, and a retention index of 0.6838. As shown in the consensus tree of the 16 most parsimonious trees, the resolution of the second analysis is better than that of the first, with the interrelationships of more non-marine groups established (Fig. 7b). With the exclusion of the Ichthyopterygia, interrelationships among the marine groups also changed, especially for subgroups within the Sauropterygia. However, the results of the two analyses (with the inclusion or exclusion of the Ichthyopterygia) did not, as a whole, fundamentally differ in terms of the interrelationships produced by the bootstrap search.

## 6. Discussion and conclusions

Compared to *Sinosaurosphargis*, *Largocephalosaurus* is morphologically less modified from a typical diapsid reptile; it still retains an elongate body shape, a well-developed supratemporal fenestra, a suborbital fenestra (although reduced in size) and an incomplete osteoderm covering. As a group, the Saurosphargidae is also less specialized than the sister-group Sauropterygia in terms of the short neck (nine cervical vertebrae probably in all members) and the presence of the interpterygoid vacuity, the articulation between

Table 2. Changes to the data matrix of Li *et al.* (2011); character state modification, new characters, changes to coding, new characters and coding for new taxa, used to analyze the phylogenetic relationships of *Largocephalosaurus*.

### Character state modification

7. Nasals do (0) or do not (1) enter external naris. This character becomes an autapomorphy of some *Cymatosaurus* with the nasal being absent in *Augustasaurus*, *Pistosaurus*, and plesiosaurs. As such, the character is uninformative, and hence ignored in the analysis of Li *et al.* (2011). The nasal is present in the pistosaur *Yunguisaurus* and informative as the latter is included in this analysis.
13. Upper temporal fenestra absent (0), or present and subequal in size or slightly larger than the orbit (1), or present and distinctly larger than orbit (2), or present and distinctly smaller than orbit (3), or secondarily closed or nearly closed (4).
66. Transverse processes of neural arches of the dorsal region relatively short (0), or distinctly elongated and narrow, narrower than the space between the transverse processes (1), or distinct elongate and broad, much broader than the space between the transverse processes (2), or extremely long, extending laterally to the margin of the trunk (3). State 3 is seen in *Cyamodus hildegardis* (Scheyer, 2010, fig. 10).
88. Coracoid of rounded contours with a foramen entirely in the bone (0), slightly waisted (1), strongly waisted (2), with expanded medial symphysis and ridge-like thickening of the bone extending from glenoid facet posteriorly along lateral edge of the bone, coracoid foramen not enlarged (3), with expanded medial symphysis and ridgelike thickening of the bone extending from glenoid facet transversely through the bone, coracoid foramen much enlarged (4), rounded or nearly rounded contours with a foramen laterally open (5).
99. Iliac blade well developed (0), reduced but projecting beyond level of posterior margin of acetabular portion of ilium (1), reduced and no longer projecting beyond posterior margin of acetabular portion of ilium (2), or absent, i.e. reduced to simple dorsal stub (3), or elongate shaft (4) (Sato *et al.* 2010).
101. Obturator foramen closed (0) or open (1) in adult. The thalattosaur coding is based on *Askeptosaurus* or absent (2) (Sato *et al.* 2010).
119. The medial gastral rib element always has only a single (0) lateral process, or may have a two-pronged lateral process on one side (1), or contributes to the formation of the plastron (2) (for Testudines and *Odontochelys*, after Wu *et al.* 2011).
132. Fewer (0), or more (1) than 30 cervical vertebrae, or more than 40 (2).
140. Neural canal evenly proportioned (0), distinctly higher than wide (1) or wider than high (2) in *Saurosphargis* (see Nosotti & Rieppel, 2003, fig. 11 below) and *Sinosauropsphargis* (see Li *et al.* 2011, fig. 3A).
141. Dorsal ribs without (0), or with distinct, fan-shaped uncinat process on the convex margin (1), or on the concave margin (2), or with a distinct crest on the dorsal surface of the shoulder region (3).

### Two new characters

158. Lateral most elements of gastral sets widely spaced (0) or closely associated with each other (1) or joining in the formation of plastron (2).
159. Premaxilla does (0), or does not (1) enter the external naris.

### Character state coding change in some taxa

- Odontochelys*: character 31 from '0' to '?' because the state unknown; 56 from '0' to '1' because the maxilla does not bear one or two caniniform teeth; 57 from '1' to '0' because the maxillary tooth row restricted to a level in front of the posterior margin of the orbit; 82 from '?' to '1' because a disarticulated interclavicle is roughly T-shaped (see IVPP V 15653); 87 from '2' to '0' because of only one ossification of the coracoid and no state 2 defined for this character; 119 from '?' to '2' because the medial gastral rib element contributing to the formation of the plastron (modified as in Wu *et al.* 2011); 126 from '0' to '1' because the distal end of ulna distinctly expanded.
- Choristodera*: character 12 from '2' to '02' because preorbital and postorbital region of skull subequal length in early forms such as *Hyphalosaurus*; 137 from '1' to '01' because snout relatively short, rounded in early forms such as *Hyphalosaurus* (see Gao & Ksepka, 2008).
- Anaro-Dactylo*: character 23 from '?' to '0' because jugal extends anteriorly along the ventral margin of the orbit in new specimen (see Klein, 2009).
- Cyamodus*: character 66 from '1' to '3' because the transverse process is dorsoventrally broad and extremely elongate, extending laterally and approaching the margin of the trunk (see Scheyer, 2010, fig. 10).
- Plesiosaurus*: character 8 from '?' to '2' because paired nasal separated from one another by nasal processes of the premaxillae extending back to the frontal bone (see Storrs, 1997); 99 from '2' to '4' (new from Sato *et al.* 2010); 132 from '1' to '2' because of more than 40 cervical vertebrae (modified).
- Eusauropsphargis*: (BES\_SC\_390): character 88 from '0' to '5' because a nearly round coracoid with an open foramen (new); 145 from '0' to '1' because dorsal ribs transversely broadened. *Saurosphargis*: character 66 from '1' to '2' because transverse processes of neural arches of the dorsal region relatively distinct elongate and broad, much broader than the space between the transverse processes (new); 140 from '?' to '2' because neural canal wider than high (see Nosotti & Rieppel, 2003, fig.11); 141 from '0' to '2' because dorsal ribs with distinct, fan-shaped uncinat process on the concave margin (new); 149 from '0' to '?' because no evidence for the marginal teeth with concave lingual surface of crown.
- Sinosauropsphargis*: character 12 changed from '0' to '1' because preorbital region is distinctly longer than the postorbital region; 22 from '1' to '0' because the supratemporal present; 36 from '?' to '0' because the occipital crest absent; 56 from '0' to '1' because one or two caniniform teeth absent; 61 from '0' to '1' because dorsal intercentra absent; 66 from '1' to '2' because transverse processes of neural arches of the dorsal region relatively distinct elongate and broad, much broader than the space between the transverse processes (modified); 73 from '?' to '0' because of two sacral ribs; 74 from '?' to '1' because sacral ribs without distinct expansion of distal head; 75 from '?' to '0' because sacral (and caudal) ribs or transverse processes sutured to their respective centrum; 83 from '?' to '2' because posterior process on (T-shaped) interclavicle rudimentary or absent; 105 from '?' to '1' because internal trochanter reduced; 119 from '0' to '1' because the medial gastral rib element may have a two-pronged lateral process on one side; 140 from '0' to '2' because neural canal wider than high (modified).

### New taxa with character state coding

*Largocephalosaurus qianensis*: 1000000020 0130110311 100011201? ?01?000010 0?12?0?100 1100010110 1101?10100 01010110? 112111051? 0121101110 11?0011?10 0011000010 000001001? 00?0011010 2000200010 000000011

*Largocephalosaurus polycarpon* (based on not only the skull but also the newly prepared postcranial skeleton, as such there are coding changes in many characters in relation to Cheng *et al.* 2012): 1001000020 0130111311 100011201? ? 01?? 000?0 ??????110? ??00010?1? 11?1?1?100 0111011?0 ?1?1?0??? 01??121110 ???0011111 0011000?10 0000?1?00? 00?001101? 30002???10 000000011

*Yunguisaurus* (based on the type specimen from Sato *et al.* 2010 and the referred specimen from Zhao *et al.* 2008 and pers. obs.): 101?010220 02?01?33? ???0?1201? ??1???02?? ?202?00110 2001?0110 1101101?0? 10100?1?? ????11?3?? 011113124? 21?01?1?10 01??000??1 02??11000? ?211201110 0100000000 000000000

the braincase and palate, the pronounced transverse process of the pterygoid and the ectopterygoid.

The monophyly of the Saurosphargidae is well supported by 20 synapomorphies including 13 un-

equivocal character states (see Fig. 7). There are seven synapomorphies (with two unequivocal character states: the transverse processes of the dorsal vertebrae distinctly elongate and broad, much broader than spaces

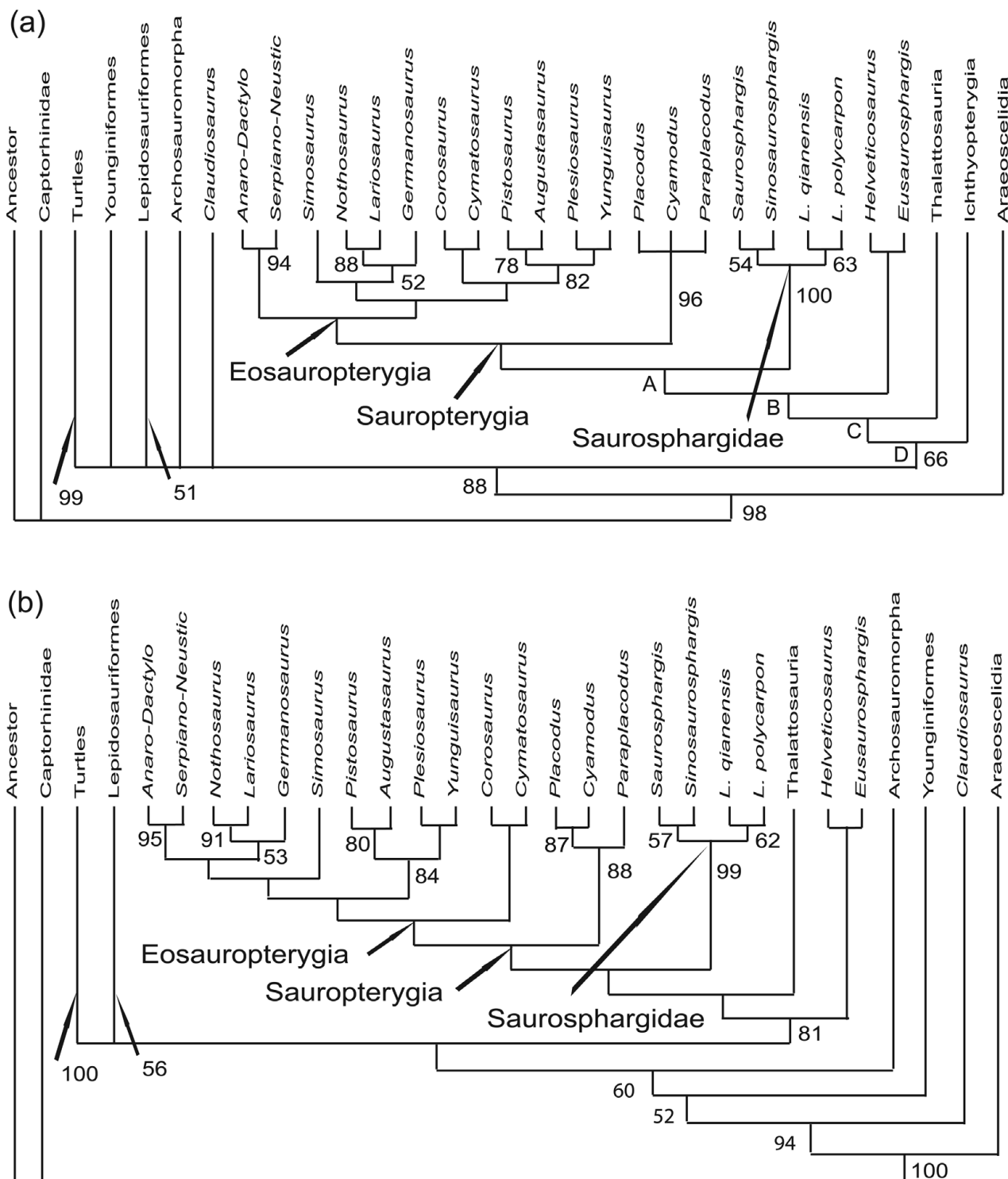


Figure 7. Strict consensus trees of (a) 11 most parsimonious trees (MPTs) of the analysis with all taxa included; and (b) 16 MPTs of the analysis with the exclusion of Ichthyopterygia. Arabic numbers indicate the bootstrap support values; clades without numbers have a bootstrap support value lower than 50%. Abbreviations: *Anaro* – *Anarosaurus*; *Dactylo* – *Dactylosaurus*; *Serpiano* – *Serpianosaurus*; *Neustic* – *Neusticosaurus*. Synapomorphies, as optimized under accelerated transformation (ACCTRAN) assumptions in tree 1 of the 11 MPTs obtained in the first analysis (\* indicates unequivocal character state): Sauropterygia, character states 13 (2)\*, 18(0)\*, 22(1), 29(0)\*, 41(1), 43(0)\*, 51(2)\*, 54(1)\*, 73(1), 78(1)\*, 95(0)\*, 98(2)\*, 115(1), 135(1), 142(1), 147(1); Saurosphargidae, character states 12(1), 16(1), 25(1)\*, 33(1)\*, 38(0), 63(0)\*, 68(1)\*, 71(0), 72(1)\*, 74(1)\*, 85(1), 93(2)\*, 104(0), 119(1)\*, 126(1)\*, 136(1)\*, 141(2), 145(2)\*, 149(1)\*, 158(1)\*; A, character states 17(2), 49(0), 51(1), 81(1)\*, 83(2)\*, 84(1), 90(1), 92(2)\*; B, character states 37(0), 42(1), 66(1)\*, 89(1)\*, 98(1), 99(1), 101(1)\*; C, character states 9(2), 29(1), 31(1)\*, 38(1), 45(1)\*, 48(1)\*, 49(1), 62(1), 64(1), 97(1), 139(1); D, character states 1(1)\*, 9(0), 12(0), 13(3)\*, 18(3)\*, 58(1)\*, 61(1)\*, 75(0), 98(2)\*, 102(1)\*, 105(1)\*, 109(1), 110(1), 112(0), 113(1), 114(1), 137(1)\*.

between the transverse processes [character 66] and the neural canal distinctly wider than high [character 140]) to support the close relationship of *Saurosphargis*

with *Sinosaurosphargis*, while four synapomorphies (including three unequivocal character states: the parietal skull table weakly constricted [character 19],

the internal trochanter well developed, [character 105] and the premaxilla excluded from the external naris [character 159]) support the monophyly of *Largocephalosaur* itself (see Fig. 7). It is obvious that the fragmentary nature of *Saurosphargis* has obscured the consistency index of the other synapomorphies shared with *Sinosaurosphargis* and those for *Largocephalosaur*. As for the close affinity of the Saurosphargidae to the Sauropterygia rather than thalattosaurs, eight synapomorphies are recognized, of which three are unequivocal, all with a consistency index of 0.5 or 1.0: the clavicle applied to the anteromedial surface of the scapula, [character 81(1)]; the posterior process of boomerang-like or atypical T-shaped interclavicle rudimentary [character 83(2)] and the humerus curved [character 92(1)]. The clavicle was described by Li *et al.* (2011) as articulating with the anterolateral surface of the scapula in *Sinosaurosphargis*. As argued earlier, based on our further examination of the specimen, the clavicle is also applied to the anteromedial surface of the scapula in this genus.

Although the bootstrap values are higher than 50 % for the clades of the turtles (100 %) and Lepidosauromorpha (57 %), interrelationships between them as well as with the Archosauromorpha, Younginiformes, *Claudiosaurus* and the clade including all marine reptilian groups are unresolved in this study. Interestingly, the addition of *Largocephalosaur* and *Yunguisaurus* did not change much in terms of the interrelationships within the clade of all related marine reptilian groups but significantly alters the phylogenetic positions of the turtles, Lepidosauromorpha, and Archosauromorpha. This, as suggested by Cheng *et al.* (2012b), may have been related to the unbalance of the current data matrix that mainly focuses on the marine reptiles. It is also interesting that the Ichthyopterygia did not play a significant role in establishing the interrelationships among the included aquatic groups, which is in sharp contrast to the findings of Li *et al.* (2011).

As indicated by the low bootstrap values, the interrelationships recognized here for all marine reptilian groups are not very stable and may alter with the discovery of new forms or better specimens of those fragmentary taxa. One of the most striking characteristic features of the Saurosphargidae is the dorsal osteoderm covering, which sometimes forms a closed carapace; among other marine reptilian groups, a similar situation is present in only the Placodontia, the basal group of the Sauropterygia. Recent studies of the placodontian phylogeny (such as Rieppel, 2000b) have indicated that the closed dorsal carapace was formed in the derived members of the Placodontia, which implies that this characteristic novelty may have independently evolved in the two groups.

**Acknowledgements.** We are deeply grateful to Mr Jinzhao Ding and Yinfang Chen (IVPP) and Ms Tian-fen Hu (GMPKU) for the preparation of the specimens and to Mr Wei Gao (IVPP) for taking the photos. X.-C.W particularly wishes to thank the IVPP for hospitality during his visit. T. Sato and an anonymous referee carefully reviewed the manuscript,

offering critical comments and suggestions that led to its great improvement. This work was supported by research grants from the National Natural Science Foundation of PR China (NNSFC-41072014 and 40772015 to CL and X-CW; 40920124002 and 40672002 to D-YJ), the CAS/SAFEA International Partnership Program for Creative Research Teams of China (to CL and X-CW), the Program for New Century Excellent Talents in Universities (NCET-07-0015 to D-YJ), CMN (to X-CW), and FMNH (to OR).

## References

- CARROLL, R. L. & GASKILL, P. 1985. The nothosaur *Pachypleurosaurus* and the origin of plesiosaurs. *Philosophical Transactions of the Royal Society of London B* **309**, 343–93.
- CHENG, L., CHEN, X., ZENG, X. & CAI, Y. 2012a. A new eosauropterygian (Diapsida: Sauropterygia) from the Middle Triassic of Luoping, Yunnan Province. *Journal of Earth Science* **23**, 33–40.
- CHENG, Y.-N., SATO, T., WU, X.-C. & LI, C. 2006. First complete pistosauroid from the Triassic of China. *Journal of Vertebrate Paleontology* **26**, 501–4.
- CHENG, Y.-N., WU, X.-C., SATO, T. & SHAN, S.-Y. 2012b. A new eosauropterygian (Diapsida: Sauropterygia) from the Triassic of China. *Journal of Vertebrate Paleontology* **32**, 1335–49.
- GAO, K. & KSEPKA, D. T. 2008. Osteology and taxonomic revision of *Hyphalosaur* (Diapsida: Choristodera) from the Lower Cretaceous of Liaoning, China. *Journal of Anatomy* **212**, 737–68.
- HUENE, F. VON 1936. *Henodus chelyops*, ein neuer Placodontier. *Palaeontographica A* **84**, 99–148.
- JIANG, D. Y., MOTANI, R., HAO, W.-C., RIEPPEL, O., SUN, Y.-L., TINTORI, A., SUN, Z.-Y. & SCHMITZ, L. 2009. Biodiversity and sequence of the Middle Triassic Panxian marine reptile fauna, Guizhou Province, China. *Acta Geologica Sinica* **83**, 451–59.
- JIANG, D.-Y., RIEPPEL, O., MOTANI, R., HAO, W.-C., SUN, Y.-L., SCHMITZ, L. & SUN, Z.-Y. 2008. A new Middle Triassic eosauropterygian (Reptilia, Sauropterygia) from Southwestern China. *Journal of Vertebrate Paleontology*, **28**, 1055–62.
- JIANG, D.-Y., RIEPPEL, O., MOTANI, R., HAO, W.-C. & TINTORI, A. 2011. Marine reptile *Saurosphargis* from Anisian (Middle Triassic) of Panxian, Guizhou, southwestern China. *Journal of Vertebrate Paleontology* **31**(Supplement 2), 132.
- JIANG, D.-Y., SCHMITZ, L., HAO, W.-C. & SUN, Y.-L. 2006. A new mixosaurid ichthyosaur from the Middle Triassic of China. *Journal of Vertebrate Paleontology* **26**, 60–9.
- KLEIN, N. 2009. Skull morphology of *Anarosaurus heterodontus* (Reptilia: Sauropterygia: Pachypleurosauria) from the Lower Muschelkalk of the Germanic Basin (Winterswijk, the Netherlands). *Journal of Vertebrate Paleontology* **29**, 665–76.
- LI, C., RIEPPEL, O., WU, X.-C., ZHAO, L.-J. & WANG, L.-T. 2011. A new Triassic marine reptile from Southwestern China. *Journal of Vertebrate Paleontology* **31**, 303–12.
- LIU, J., RIEPPEL, O., JIANG, D.-Y., AITCHISON, J. C., MOTANI, R., ZHANG, Q.-Y., ZHOU, C.-Y. & SUN, Y.-Y. 2011. A new pachypleurosaur (Reptilia: Sauropterygia) from the lower Middle Triassic of southwestern China and the phylogenetic relationships of Chinese pachypleurosaur. *Journal of Vertebrate Paleontology* **31**, 291–302.
- MOTANI, R., JIANG, D.-Y., TINTORI, A., SUN, Y.-L., HAO, W.-C., BOYD, A., HINIC-FRLOG, S., SCHMITZ, L., SHIN,

- J.-Y. & SUN, Z.-Y. 2008. Horizons and assemblages of Middle Triassic marine reptiles from Panxian, Guizhou, China. *Journal of Vertebrate Paleontology* **28**, 900–3.
- NICHOLLS, E. 1999. A re-examination of *Thalattosaurus* and *Nectosaurus* and the relationships of the Thalattosauria (Reptilia: Diapsida). *PaleoBios* **19**, 1–31.
- NOSOTTI, S. & RIEPPEL, O. 2003. *Eusaurosphargis dalsassoi* n. g. n. sp., a new, unusual diapsid reptile from the Middle Triassic of Besano (Lombardy, N Italy). *Memorie della Società italiana di Scienze naturali e del Museo Civico di Storia Naturale di Milano* **31**, 1–33.
- OSBORN, H. F. 1903. On the preliminary division of the Reptilia into two sub-classes, Synapsida and Diapsida. *Science* **17**, 275–6.
- RIEPEL, O. 1989. A new pachypleurosaur (Reptilia: Sauropterygia) from the Middle Triassic of Monte San Giorgio, Switzerland. *Philosophical Transactions of the Royal Society of London B* **323**, 1–73.
- RIEPEL, O. 1998a. The systematic status of *Hanosaurus hupehensis* (Reptilia, Sauropterygia) from the Triassic of China. *Journal of Vertebrate Paleontology* **18**, 545–57.
- RIEPEL, O. 1998b. The status of the sauropterygian reptile genera *Ceresiosaurus*, *Lariosaurus*, and *Silvestrosaurus* from the Middle Triassic of Europe. *Feldiana* **38**, 1–46.
- RIEPEL, O. 1999. The sauropterygian genera *Chinchenia*, *Kwangsisaurus*, and *Sanchiaosaurus* from the Lower and Middle Triassic of China. *Journal of Vertebrate Paleontology* **19**, 321–37.
- RIEPEL, O. 2000a. Sauropterygia I: Placodontia, Pachypleurosauria, Nothosauroida, Pistosauroida. *Encyclopedia of Paleoherpetology* **12A**, 1–134.
- RIEPEL, O. 2000b. *Paraplocodus* and the phylogeny of the Placodontia (Reptilia: Sauropterygia). *Zoological Journal of the Linnean Society* **130**, 635–59.
- SANDER, P. M. 1989. The pachypleurosaurids (Reptilia: Nothosauria) from the Middle Triassic of Monte San Giorgio, (Switzerland), with the description of a new species. *Philosophical Transactions of the Royal Society of London B* **325**, 561–670.
- SATO, T., CHENG, Y.-N., WU, X.-C. & LI, C. 2010. Osteology of *Yunguisaurus* Cheng et al., 2006 (Reptilia; Sauropterygia), a Triassic pistosauroid from China. *Paleontological Research* **14**, 179–95.
- SCHEYER, T. M. 2010. New interpretation of the postcranial skeleton and overall body shape of the placodont *Cyamodus hildegardis* Peyer, 1931 (Reptilia, Sauropterygia). *Palaeontologia Electronica* **13**, 13.2.15A.
- SHANG, Q.-H., WU, X.-C. & LI, C. 2011. A new eosauropterygian from the Middle Triassic of eastern Yunnan Province, southwestern China. *Vertebrata Palasiatica* **49**, 155–73. [Chinese 155; English 156–73]
- SUN, Z.-Y., HAO, W.-C., SUN, Y.-L. & JIANG, D.-Y. 2006. Conodont evidence for the age of the Triassic Panxian fauna, Guizhou. *Acta Geologica Sinica* (English edition) **80**, 621–30.
- STORRS, G. W. 1991. Anatomy and relationships of *Corosaurus alcovensis* (Diapsida: Sauropterygia) and the Triassic Alvova Limestone of Wyoming. *Bulletin of Peabody Museum of Natural History* **44**, 1–151.
- STORRS, G. W. 1997. Morphological and taxonomic clarification of the genus *Plesiosaurus*. In *Ancient Marine Reptiles* (eds J. M. Callaway & E. L. Nicholls), pp. 145–190. Academic Press, 501pp.
- SWOFFORD, D. L. 2002. *PAUP\* 4.0b10. Phylogenetic Analysis Using Parsimony (\*and other methods)*. Sinauer Associates, Sunderland, Massachusetts, 199 pp.
- WANG, X. F., CHEN, X. H., CHEN, L., WANG, C. S., BACHMANN, G. H., SANDER, M. & HAGDORN, H. 2009. Sedimentary and palaeoecological environments of the Guanling and related biotas. *Acta Palaeontologica Sinica* **48**, 509–26.
- WU, X.-C., CHENG, Y.-N., SATO, T. & SHAN, H.-Y. 2009. *Miodentosaurus brevis* Cheng et al., 2007 (Diapsida: Thalattosauria): its postcranial skeleton and phylogenetic relationships. *Vertebrata Palasiatica* **47**, 1–20.
- WU, X.-C., CHENG, Y.-N., LI, C., ZHAO, L.-J. & SATO, T. 2011. New information on *Wumengosaurus delicatmandibularis* Jiang et al., 2008 (Diapsida: Sauropterygia), with revision of the osteology and phylogeny of the taxon. *Journal of Vertebrate Paleontology* **31**, 70–83.
- ZHANG, Q.-Y., ZHOU, C. Y., LU, T., LOU, X.-Y., LIU, W., SUN, Y.-Y., HUANG, J.-Y. & ZHAO, L.-S. 2009. A conodont-based Middle Triassic age assignment for the Luoping Biota of Yunnan, China. *Science in China Series D: Earth Sciences* **52**, 1673–8.